OPEN ACCESS

KING'S College LONDON

King's Research Portal

DOI:
10.2337/db17-0021

Document Version
Peer reviewed version

Link to publication record in King's Research Portal

Citation for published version (APA):
Kronenberg-Versteeg, D., Eichmann, M., Russell, M. A., de Ru, A., Hehn, B., Yusuf, N., van Veelen, P. A., Richardson, S. J., Morgan, N. G., Lemberg, M. K., & Peakman, M. (2018). Molecular Pathways for Immune Recognition of Preproinsulin Signal Peptide in Type 1 Diabetes. *Diabetes*, *67*(4), 687-696. https://doi.org/10.2337/db17-0021

Citing this paper
Please note that where the full-text provided on King's Research Portal is the Author Accepted Manuscript or Post-Print version this may differ from the final Published version. If citing, it is advised that you check and use the publisher's definitive version for pagination, volume/issue, and date of publication details. And where the final published version is provided on the Research Portal, if citing you are again advised to check the publisher's website for any subsequent corrections.

General rights
Copyright and moral rights for the publications made accessible in the Research Portal are retained by the authors and/or other copyright owners and it is a condition of accessing publications that users recognize and abide by the legal requirements associated with these rights.

•Users may download and print one copy of any publication from the Research Portal for the purpose of private study or research.
•You may not further distribute the material or use it for any profit-making activity or commercial gain
•You may freely distribute the URL identifying the publication in the Research Portal

Take down policy
If you believe that this document breaches copyright please contact librarypure@kcl.ac.uk providing details, and we will remove access to the work immediately and investigate your claim.

Download date: 27. Dec. 2024

Molecular pathways for immune recognition of preproinsulin signal peptide in type 1 diabetes

Running title: Preproinsulin processing for immune recognition

Deborah Kronenberg-Versteeg[1,2,3]*†, Martin Eichmann[1]*, Mark A. Russell[4], Arnoud de Ru[5], Beate Hehn[6], Norkhairin Yusuf[1], Peter A. van Veelen[5], Sarah J. Richardson[4], Noel G. Morgan[4], Marius K. Lemberg[6], Mark Peakman[1,2]

[1]Department of Immunobiology, Faculty of Life Sciences & Medicine, King's College London, London, UK
[2]National Institute for Health Research, Biomedical Research Centre at Guy's and St Thomas' Hospital Foundation Trust and King's College London, London, UK
[3]current address: Wellcome Trust – Medical Research Council Stem Cell Institute, University of Cambridge, Cambridge, UK
[4]Institute of Biomedical & Clinical Science, University of Exeter Medical School, Exeter EX2 5DW, UK
[5]Department of Immunohematology and Blood Transfusion, Leiden University Medical Center, Leiden, The Netherlands
[6]Center for Molecular Biology of Heidelberg University (ZMBH), DKFZ-ZMBH Alliance, Heidelberg, Germany

* These authors contributed equally to this work

†Corresponding author:
Dr Deborah Kronenberg-Versteeg, dk480@cam.ac.uk
Wellcome Trust – MRC Stem Cell Institute, University of Cambridge, Tennis Court Road, Cambridge CB2 1QR. Telephone +44-(0)1223760213

Word count: 3965 (not including list of abbreviations)

Number of tables: 1

Number of figures: 6

Diabetes Publish Ahead of Print, published online January 17, 2018

Abstract

The signal peptide region of preproinsulin (PPI) contains epitopes targeted by human leucocyte antigen-A (HLA-A)-restricted (HLA-A0201, A2402) cytotoxic T-cells as part of the pathogenesis of β-cell destruction in type 1 diabetes. We extended PPI epitope discovery to disease-associated *HLA-B*1801 and HLA-B*3906* (risk) and *HLA-A*1101 and HLA-B*3801* (protective) alleles revealing that 4/6 alleles present epitopes derived from the signal peptide region. During co-translational translocation of PPI, its signal peptide is cleaved and retained within the endoplasmic reticulum (ER) membrane, implying it is processed for immune recognition outside of the canonical, proteasome-directed pathway. Using *in vitro* translocation assays with specific inhibitors and gene knockout in PPI-expressing target cells we show that PPI signal peptide antigen processing requires signal peptide peptidase (SPP). The intramembrane protease SPP generates cytoplasm-proximal epitopes, which are transporter-associated-with–antigen-processing (TAP)-dependent, and ER-luminal (TAP-independent) epitopes, each presented by different HLA class I molecules, and N-terminal trimmed by ER aminopeptidase 1 (ERAP1) for optimal presentation. *In vivo*, TAP expression is significantly up-regulated and correlated with HLA class I hyper-expression in insulin-containing islets of patients with type 1 diabetes. Thus, PPI signal peptide epitopes are processed by SPP and loaded for HLA-guided immune recognition via pathways that are enhanced during disease pathogenesis.

	abbreviation
(Z-Leu-Leu-NHCH2)2CO	$(Z\text{-}LL)_2$ ketone
7-Aminoactinomyocin D	7-AAD
beta-2-microglobulin	B2M
cluster of differentiation	CD
clustered regularly interspaced short palindromic repeats	CRISPR
cytotoxic T lymphocyte	CTL
endoplasmic reticulum	ER
endoplasmic reticulum aminopeptidase	ERAP
enzyme-linked immunosorbent assay	ELISA
formalin-fixed paraffin embedded	FFPE
glyceraldehyde 3-phosphate dehydrogenase	GAPDH
human leucocyte antigen	HLA
Islet amyloid polypeptide	IAPP
Insulin-containing islet	ICI
insulin degrading enzyme	IDE
knock out	Ko
macrophage inflammatory protein-1β	MIP-1β
major histocompatibility complex	MHC
mean fluorescence intensity	MFI
messenger RNA	mRNA
peptide loading complex	PLC
preproinsulin	PPI
signal peptide	SP
signal peptide peptidase	SPP
small interfering RNA	siRNA
sodium dodecyl sulfate polyacrylamide gel electrophoresis	SDS-PAGE
standard error of the mean	SEM
TAP binding protein	TAPBP
threshold cycle	Ct
transporter associated with antigen processing	TAP

Introduction

In type 1 diabetes, immune-mediated destruction of insulin-producing β-cells is the pathological process leading to insulin deficiency and hyperglycaemia (1). Multiple arms of the immune system are likely to contribute to this tissue-damaging process, with strong indications that CD8+ cytotoxic T lymphocytes (CTLs), are a dominant killing pathway. Evidence includes a data from preclinical models showing dependence of disease development on intact CD8/MHC class I mechanisms (2), supported by compelling findings in human studies, including the existence of high-risk polymorphic HLA class I genes (3); enrichment of effector CTLs specific for β-cell targets in the circulation in new-onset disease (4; 5); recapitulation of β-cell killing by patient-derived preproinsulin (PPI)-specific CTLs *in vitro* (4; 6); CD8 T cell dominance of islet infiltrates in patients, including the presence of CD8s bearing receptors specific for β-cell autoantigens (7; 8); hyper-expression of HLA class I both at the RNA and protein level in residual insulin containing islets (ICIs) in type 1 diabetes pancreatic tissue (9); and recent success in halting β-cell loss using immunotherapy targeted at effector CD8 T cells (10).

The potential for the immunological dialogue between CTLs and β-cells to be a key component of the development of type 1 diabetes has led several groups to focus on the relevant molecular interactions that govern this interface, including studies on HLA class I gene polymorphisms carrying modified risk of disease (*HLA-A*0201, A*1101, A*2402, B*1801, B*3801* and *B*3906* (3; 11; 12)) and antigenic targets within β-cells recognized by CTLs. These have especially focused on PPI which is considered a primary target in β-cell autoimmunity because anti-insulin autoantibodies are frequently the first disease manifestation in high-risk children (12).

For immune recognition, processing and presentation of peptides by MHC class I commonly results from degradation of proteins by the proteasome (13), generating cytosolic peptides of 8-16 amino acids (14) which are transported into the endoplasmic reticulum (ER) lumen via transporter associated with antigen processing (TAP) (15), part of the MHC class I peptide loading complex (PLC; (16)). ER aminopeptidase 1 (ERAP1) trims peptides to a suitable length for MHC loading if required (17), and peptide-MHC complexes are delivered to the cell surface for immune recognition. Proteasome-independent, cytoplasm-based non-canonical antigen presentation pathways have also been described (18). Whereas these and the canonical route collectively require TAP for peptide delivery into the ER, signal peptide epitopes from secretory proteins may be MHC-loaded independently of TAP (19) following signal peptidase cleavage and intramembrane proteolysis by signal peptide peptidase (SPP) (20-22). Interestingly, peptides originating from the ER luminal side of the signal peptide can access the PLC directly (23-25), whereas epitopes close to the cytosol may require proteasomal trimming and TAP for ER entry (26). However, the extent to which signal peptides and these non-canonical epitope-generation pathways fuel immune recognition of single antigens and play a role in physiological responses remains unclear.

The present study was motivated by the need for a better understanding of autoantigen processing for immune recognition of β-cells via these different routes, which could provide novel insights into disease pathogenesis and highlight pathways susceptible to therapeutic manipulation. We previously reported that the predominant epitope species presented to CTLs by human cell lines co-transfected with the *INS* gene (encoding PPI) and the HLA class I genes *HLA-A*0201* and *A*2402* derived from the signal peptide region (4; 6). These signal peptide-derived epitopes are recognized by patient CTLs and presented by β-cells bearing the relevant HLA class I molecule. Here we examine whether PPI signal peptide is a more general source of epitopes by studying additional HLA class I molecules associated with type

1 diabetes. We show that generation of epitopes from the PPI signal peptide is driven by the intramembrane protease SPP, and that loading into nascent HLA class I molecules requires trimming by ERAP1 and is either direct or follows cytoplasmic translocation and TAP, with the selected pathway being determined by HLA allele. Importantly, we show that the key factors ERAP1 and TAP are expressed in insulin-containing islets of patients studied post mortem after type 1 diabetes diagnosis, indicating that the multiple pathways that are potentially critical in the CTL:β-cell dialogue are active in the disease setting.

Methods

Cell lines and epitope discovery

K562 cells transfected with *HLA-A*1101, HLA-B*1801, HLA-B*3801, or HLA-B*3906* and PPI cDNAs (K562-HLA-PPI cells) were generated as described (4). Expression of HLA class I was confirmed by flow cytometry (anti-HLA-ABC antibody W6/32; Serotec, Oxford, U.K.). Proinsulin was detected in supernatants by ELISA (DRG International, Marburg, Germany). Subsequently, ~10^{10} cells from each cell line were harvested and immunoaffinity purification of HLA-A1101, HLA-B1801, HLA-B3801 and HLA-B3906, peptide extraction and nano high-performance liquid chromatography–mass spectrometry performed as described (4; 6; 27; 28).

Inhibitors, RNA interference and T cell clone activation

K562-A24-PPI cells were transfected twice within 48 hours with 20nM small interfering RNAs (Applied Biosystems, Foster City, Ca, USA) targeting B2M (#s1852), ERAP1 (#s28618), ERAP2 (#s34520), TAP1 (#s13778, #s13780), TAP2 (#s13781, #s13782, #s13783) using Lipofectamine RNAiMAX (Invitrogen, Paisley, U.K.). Knockdown was assessed by RT-PCR using TaqMan specific primers and relative cDNA content normalized to *GAPDH* gene expression. CD8 T cell clones for $PPI_{3\text{-}11}$-HLA-A2402 and $PPI_{15\text{-}24}$-HLA-A0201 (4; 6) were co-cultured with K562-HLA-PPI target cells at indicated effector:target ratios (4 hours) and response measured as degranulation (CD107a expression (29)) or MIP-1β release (R&D systems, Minneapolis, MN, USA).

Site directed mutagenesis

To alter single or multiple amino acids (as highlighted in **Supplementary Table 1**), PPI-containing plasmid pcDNA3/PPI was amplified using altered primers (PPI9P→L, CCC→CTC; PPI12A→L, GCG→CTG; PPI15A→L, GCC→CTC; with 18-20 nucleotide

overhang preceding and following the mutated site) and PfuTurbo DNA Polymerase AD (Agilent, Santa Clara, CA, USA) with sequence confirmation before use.

In vitro transcription, translation and translocation and analysis of SPP processing

Plasmid pcDNA3/PPI was linearized with *EcoRI* and transcribed *in vitro* with T7 RNA polymerase at 42°C using 500μM m7G(5′)ppp(5′)G CAP analogue (New England Biolabs, Ipswich, MA, USA) (30). mRNAs were translated *in vitro* in 25μl rabbit reticulocyte lysate (Promega, Madison, WI, USA) containing [^{35}S]-methionine and [^{35}S]-cysteine (Perkin Elmer, Waltham, MA, USA) and, where indicated, 2 equivalents of nuclease-treated dog pancreas rough microsomes (31). $(Z\text{-}LL)_2$-ketone (SPP inhibitor, 5μM; Merck-Calbiochem, San Diego, CA, USA) or DMSO control were added as indicated. After 30 minutes at 30°C, microsomes were extracted with 500mM KOAc, solubilized in SDS-sample buffer (32) and analysed by SDS-PAGE using Tris-bicine-urea acrylamide gels (15% T, 5% C; 8 M urea) (33) and an FLA 7000 phosphorimager (Fuji) with Multi Gauge software (Fuji). Translations of reference peptide comprising the 24-amino acid PPI signal sequence was performed in wheat germ extract (34).

Immunohistochemistry and Immunofluorescence

Formalin-fixed paraffin embedded (FFPE) pancreas sections from 6 controls and 6 type 1 diabetes cases (Exeter Archival Diabetes Biobank; http://foulis.vub.ac.be/; **Supplementary Table 2**; ethical approval 15/W/0258) were studied by immunohistochemistry. Sections were dewaxed, rehydrated and heated by microwave (800W) for 20 minutes, blocked in 5% normal goat serum before incubation with primary and secondary antibodies (**Supplementary Table 3**), haematoxylin counter-stain, dehydration and mounting in a distyrene/xylene-based mountant (DPX). Multiple antigens within the same FFPE section were probed in a sequential manner with up to three different antibodies (**Supplementary**

Table 3) and images captured (Leica AF6000 microscope, Milton Keynes, U.K.). Mean fluorescence intensity (MFI) of stained antigens was analysed using ImageJ and isotype control antisera used to confirm reagent specificity.

SPP knockout using CRISPR

CRISPR guide sequences for exons of SPP (gene name *HM13*) were designed using CRISPR DESIGN tool (www.crispr.mit.edu) (**Supplementary Table 4**) and cloned into pLG2C vector containing eGFP linked to a Cas9 cassette via P2A. K562-A2-PPI were transfected with each of two pLG2C vectors (containing guide sequence for Exon 2 or 3 and Exon 10 or 11) or empty vector (mock treated: no guide sequence) using Effectene (Qiagen, Hilden, Germany). Single cells sorted for high HLA-A2 (W6/32; Biolegend, San Diego, CA, UK) and eGFP were examined for gene truncation by RT-PCR and SPP amplification using primers (F: ATATATGAATTCGCACCCTCGCCATG ;R: ATATATCTCGAGGCACCAGCTGCATCATTTC) (Eurofins, Ebersberg, Germany) and Phusion High-Fidelity DNA Polymerase (New England Biolabs, Ipswich, MA, USA) and by agarose gel electrophoresis.

Results

Presentation of PPI epitopes by HLA-A1101, HLA-B1801, HLA-B3801 and HLA-B3906

K562 cells transfected with *INS* encoding human PPI and one of *HLA-A*1101, HLA-B*1801, HLA-B*3801 and HLA-B*3906* generated surrogate β-cells secreting proinsulin and expressing relevant HLA class I molecules (**Supplementary Figure 1**). The immunopeptidome eluted from affinity purified HLA-A1101 identified 905 peptides; from HLA-B1801 615 peptides; from HLA-B3801 455 peptides; and from HLA-B3906 298 peptides (all MASCOT scores ≥40) and corresponded to published HLA-binding motifs and peptide ligandomes (35). Of interest, PPI epitopes from the signal peptide region were identified for HLA-B3801, PPI_{5-14} MRLLPLLALL, and HLA-B3906, PPI_{5-12} MRLLPLLA (**Figure 1 and Supplementary Figure 2**), respectively. In addition we identified a B-chain epitope for HLA-B3801, PPI_{33-41} SHLVEALYL, and a C-peptide epitope for HLA-A1101, PPI_{80-88} LALEGSLQK. Peptide identities were confirmed by tandem mass spectrometry profiling of the synthetic compound (**Supplementary Figure 2**). No other peptides from PPI were identified.

Taken together with our previous reports of immunodominant PPI signal peptide-derived epitopes in PPI_{15-24}-HLA-A0201 (6) and PPI_{3-11}-HLA-A2402 (4), these new discoveries indicate that the signal peptide region of PPI is a rich source for processing for immune recognition (**Table 1** and **Figure 1**). To examine whether this arises because signal peptide regions are immunogenic per se, as has been reported (36), the available peptidome data was mined in greater depth, showing that the degree to which signal peptides are presented is HLA allele dependent. Whilst, for example, HLA-A0201 presents a signal peptide-derived epitope from 46% of source proteins that contain a signal peptide, for HLA-A1101 this figure is only 6.9% (**Supplementary Table 5**). Probing for any signal peptide bias using *in silico*

prediction algorithms provided similar results (**Supplementary Table 6**). We conclude that presentation of signal peptides of PPI is unlikely to result from a generalized propensity of HLA molecules to select this region for presentation, but the number of HLA molecules studied to date remains limited.

Intramembrane protease SPP cleaves PPI signal peptide

Based on previous studies of intramembrane cleavage of signal peptides (37), we hypothesized that SPP is involved in processing and cleavage of PPI signal peptide. To test this, mRNAs encoding PPI were translated *in vitro* with ER-derived microsomes and [^{35}S]-labelled methionine and cysteine. Upon insertion of PPI into microsomes, PPI signal sequence is cleaved by signal peptidase, liberating translocated proinsulin from its signal peptide (**Figure 2A**). Moreover, traces of a peptide that co-migrated with an *in vitro* translated reference peptide comprising the PPI signal sequence were detected in the membrane fraction (**Figure 2A**, compare lanes 2 and 4). Since processing of nascent chains by signal peptidase is a well-known activity in ER-derived microsomes (31), and no low molecular weight peptides were observed in the translation reaction lacking microsomes (lane 1), we conclude that the identified peptide corresponds to traces of PPI signal peptide that remain in the ER membrane fraction. In contrast, the PPI signal peptide is markedly stabilized and retained in the microsome fraction upon treatment with the SPP inhibitor (Z-LL)$_2$-ketone (**Figure 2A**, lane 3). Overall, this shows that PPI behaves as a canonical nascent chain that is processed by signal peptidase liberating a signal peptide released from the ER membrane by SPP-catalysed intramembrane cleavage.

To further study the role of intramembrane proteolysis in turnover of PPI signal peptide, amino acid residues destabilizing the helical transmembrane span surrounding the scissile peptide bond were mutated to leucine, which blocks SPP-catalysed cleavage (21). Consistent

with our previous analysis of model signal peptides, single mutation of proline (at P9) and alanine (P12 and P15) shows marginal effects on PPI signal peptide processing, whereas double mutants (9L/12L; 9L/15L; and 12L/15L) and the triple mutant (9L/12L/15L) show very marked inhibition of SPP-catalysed processing (**Figure 2B-D, Supplementary Table 1, Supplementary Figure 3**). This identifies PPI signal peptide as a *bona fide* SPP substrate and confirms the requirement for helix-breaks and limited hydrophobicity for intramembrane cleavage. Replacement of the classical helix-break residue proline at position 9 of PPI signal peptide alone is not sufficient to completely block SPP-catalysed processing and only shows effect when at least one of the nearby alanine residues, which show an intermediate stability within transmembrane helices (38), is also mutated to leucine.

We next examined whether abrogation of SPP-catalysed cleavage of PPI signal peptide impacts upon immune recognition of signal peptide-derived epitopes. Double-targeting CRISPR-Cas9 technology generated three independent K562-A2-PPI cell lines with SPP knockout (K562-A2-PPI-SPPko; SPP knockout validation shown in **Supplementary Figure 4**). When cultured with the PPI_{15-24} specific HLA-A0201-restricted CD8 T cell clone, degranulation (measures clone activation via T cell receptor ligation by peptide-HLA) frequency and magnitude were markedly reduced in the presence of K562-A2-PPI-SPPko cells compared to mock-treated lines (**Figure 3**). The difference in T cell activation is not due to differences in HLA class I expression levels (**Supplementary Figure 5**) and the SPP knockout phenotype of reduced T cell activation is rescued when cells are pulsed with cognate peptide (**Supplementary Figure 6**), These data show that SPP-catalysed processing of PPI signal peptide is an essential step to generate an immunologically relevant epitope that is implicated as having a pathogenic role in type 1 diabetes through activation of β-cell-specific autoreactive CD8 T cells (6; 8).

Requirement for proteasome, TAP and ERAP in PPI processing

We previously showed that PPI_{15-24} processing and presentation by HLA-A0201 does not require proteasome cleavage or import into the ER via TAP (6). In contrast with PPI_{15-24}-HLA-A0201, however, PPI_{3-11}-HLA-A2402 presentation is TAP dependent. RNAi inhibition of *TAP1* (94.5 +/- 2.3% mRNA knockdown) and *TAP2* (95.4 +/- 0.3% mRNA knockdown) expression in K562-A24-PPI cells markedly reduces MIP-1β production (60.7% and 30.2% respectively) by PPI_{3-11}-HLA-A2402-specific CD8 clone upon co-culture with TAP RNAi treated K562-A24-PPI cells (**Figure 4A**). This is attributable to a reduction in surface density of the specific pHLA ligand PPI_{3-11}-HLA-A2402 (TAP RNAi treated K562-A24-PPI cells show only minimal reduction in HLA class I expression; **Supplementary Figure 7**).

Next, we investigated whether ER-resident aminopeptidases are involved in the processing and presentation of PPI signal peptide epitopes. Knockdown of *ERAP1* (87.2 +/- 0.5% mRNA knockdown) in K562-A24-PPI cells by RNAi markedly reduced MIP-1β production (62.6%) by PPI_{3-11}-HLA-A2402-specific clone 4C6 , whilst no effect was seen in the presence of *ERAP2* knockdown (73.7 +/- 6.1% mRNA knockdown; 8.0% change in MIP-1β production) (**Figure 4B**). Similar effects were seen in target killing assays (data not shown). RNAi for *ERAP1* and *ERAP2* had only minimal effects on total surface HLA class I expression (**Supplementary Figure 7**), indicating that the ERAP1-mediated interference in clone 4C6 activation is likely to be an effect on target cell surface density of specific PPI_{3-11}-HLA-A2402 ligand.

TAP and ERAP1 expression in pancreas samples from subjects with type 1 diabetes

Expression of the processing proteins TAP1 and ERAP1, both of which we have shown to have potential contribution to the generation of PPI epitopes that target β-cells for killing by PPI-specific cytotoxic CD8 T cells, were investigated in human pancreas recovered from healthy control subjects and those with type 1 diabetes. TAP1 was present at low levels in the

pancreatic islets of healthy control subjects and was detected at similarly low levels in the insulin-deficient islets (IDIs) of patients with type 1 diabetes (**Figure 5A**). In contrast, TAP1 was markedly upregulated in the insulin containing islets (ICIs) of these patients (**Figure 5A**). Co-localisation studies revealed that the elevation in TAP1 expression was most evident in β-cells although it was also increased in other islet cells. Quantification of the immunostaining in six age-matched controls and six type 1 diabetes subjects was achieved by measuring the mean fluorescent intensity of TAP1 labelling in three islets from each control subject and in six islets from each patient (three ICIs and three IDIs). This confirmed a significant elevation in TAP1 expression in ICIs from type 1 diabetes patients when compared to IDIs or control islets (**Figure 5B**; $p<0.001$). Application of similar approaches demonstrated that, as previously described (9), HLA-ABC was also markedly elevated in the ICIs of type 1 diabetes patients (**Figure 5C**). Moreover, there was a strong positive correlation between the expression of TAP1 and HLA-ABC in insulin-containing islets (**Figure 5D**; $R^2= 0.519$, $p<0.001$).

ERAP1 was detected in the islets of healthy controls and was also found in the islets of donors with type 1 diabetes (**Supplementary Table 2**). However, by contrast with TAP1, ERAP1 expression was not noticeably altered between the islets of control subjects and those with type 1 diabetes (**Supplementary Figure** 8).

Model for PPI signal peptide immune processing and presentation

Collectively, these findings imply a model of PPI signal peptide processing for HLA class I presentation in which the fate that follows intramembrane cleavage is dependent upon location within the ER membrane and HLA binding potential (**Figure 6**). On the one hand, N-terminal peptides may be released into the cytoplasm, where they are dependent upon TAP transport into the ER and ERAP1 trimming, before loading into nascent HLA molecules. As

an alternative, distally generated, ER luminal peptides are directly released into the ER lumen omitting the need for TAP, but may require N-terminal trimming by ERAP1 for optimal presentation.

Discussion

In the present study, we extend our previous PPI epitope discovery effort to encompass new HLA class I alleles associated with type 1 diabetes risk/protection. This reveals PPI signal peptide as a frequent source of epitopes for multiple *HLA-A* and *-B* alleles. Our previous finding of proteasome independence for HLA-A0201 PPI presentation (6) implied a non-canonical pathway for generation of signal peptide-derived epitopes. This concept is extended in the present study, in which we highlight the requirement for intramembrane cleavage and indicate the importance of SPP in this role. We further show that following intramembrane cleavage, the pathway of peptide loading varies according to whether a signal peptide-derived epitope is N-terminal (TAP requiring) or C-terminal (TAP independent). Loading is dictated by the HLA allele and optimised in the presence of ERAP1. These findings highlight a distinct set of processing principles for PPI (stoichiometry with translation; proximity to site of HLA molecule synthesis and loading) that contrast with canonical endogenous antigen processing, which relies upon proteasome degradation of effete or damaged cytoplasmic proteins. Together with evidence that TAP expression is upregulated in relevant tissues in the disease setting, the study offers important insight into the molecular processes that are a key underpinning of interactions between cytotoxic CD8 T cells and β-cells during the pathogenesis of the disease.

One caveat in our study relates to using tumour cells transfected with the *INS* gene and selected *HLA* allele as "surrogate β-cells" to represent and understand the endogenous pathway of PPI presentation as it may occur in a human β-cell *in vivo*. It remains open to interpretation whether this approach biases epitope discovery towards a specific PPI region, although our finding of epitopes in the signal peptide, B chain and C-peptide across the different HLA molecules suggests that this is unlikely. K562 cells predominantly express the constitutive proteasome (39) whilst there is evidence that the immunoproteasome can be

upregulated in β-cells under inflammatory conditions (40) and the balance of these two could influence the spectrum of epitopes generated in human islets. Our approach is pragmatic, since obtaining sufficient, pure β-cells for such work presents a severe technical and logistical challenge. We therefore elect to conduct epitope discovery using "surrogate β-cells" and then confirm findings using human tissue. Indeed, our previous experience has been that epitopes identified in this way for HLA-A0201 and A2402 are faithful phenocopies of PPI presentation by β-cells. In both cases we were able to generate CD8 T cell clones that recognize PPI epitopes presented by both the surrogate and donor-derived β-cells. Providing similar proof for the less common alleles remains challenging, however (41), although studies examining the frequency and antigen-experience of, for example, PPI_{5-12}-B3906 and PPI_{5-14}-B3801 restricted T cells in the blood using peptide-HLA multimer technology, will provide supportive evidence of a pathogenic role.

One of our findings is to identify a non-canonical pathway of endogenous antigen processing for an epitope that is relevant to recognition of β-cells by the immune system. Central to this is an intramembrane cleavage step. Our studies conducted *in vitro* using microsomes indicate that SPP is capable of cleaving the PPI signal peptide, which is released from the ER membrane by SPP-catalysed cleavage. CRISPR-Cas9-mediated SPP knockout indicates that this enzyme is also rate-limiting for epitope generation *in vivo*. Using this and the $(Z\text{-}LL)_2$-ketone inhibitor approaches we are able to argue that SPP knockout affects processing of signal peptide, leading to reduced presentation of PPI_{15-24} and, in turn, reduced activation of the specific T cell clone. Overall this appears compelling evidence for a direct role of SPP in the processing of PPI signal peptide in a manner that is critical to the generation of this important epitope.

SPP belongs to the family of GxGD intramembrane proteases including presenilin/γ-secretase and related SPP-like proteases (37). The ER-resident SPP cleaves various signal peptides and

type II membrane proteins in a number of physiological settings (42), including the generation of a regulatory peptide from HLA-A0301 signal peptide that is required for HLA-E-mediated immunosurveillance (22). This is not the first study to draw attention to the potential requirement for intramembrane cleavage of an autoantigen in type 1 diabetes. Using algorithms to predict HLA-A0201 epitopes of islet amyloid polypeptide (IAPP), previous studies have shown CD8 T cell reactivity to $IAPP_{9-17}$ and $IAPP_{5-13}$ in the blood (43; 44) and in the case of $IAPP_{5-13}$, also in islets of patients with type 1 diabetes (8). Whether these peptides are naturally processed and presented by β-cells remains unclear, however, and if confirmed for both it would imply a complex processing pathway, since the C-terminus of $IAPP_{5-13}$ overlaps and extends into the N-terminus of $IAPP_{9-17}$.

Signal sequences are essential for protein targeting to the secretory pathway via the ER (45; 46) where, after insertion into the protein-conduction translocation channel, they are cleaved from the preprotein by signal peptidase (47), which in the case of PPI_{15-24}-HLA-A0201 also generates the epitope C-terminus. Signal peptides spanning the ER membrane require cleavage by SPP for efficient disposal (19; 20). No consensus SPP cleavage motif has been identified, beyond a strong preference for helix-destabilizing residues in the membrane spanning region (21; 48; 49), which are likely to be the proline and two alanine residues at positions 9, 12 and 15, respectively. Indeed, in our studies mutation of any one of these has a mild effect on signal peptide cleavage; any two mutations together gives a moderate phenotype; and when all three are mutated, SPP is unable to cleave, indicating that these are the helix-destabilizing residues in PPI. Once liberated, SPP-cleaved N-terminal signal peptide fragment gets access to the cytosol where it is either trimmed by the proteasome or directly loaded onto TAP and the MHC peptide-loading complex. In the case of PPI_{3-11}-HLA-A2402, we show TAP requirement, whilst PPI_{15-24}-HLA-A0201 requires neither proteasome nor TAP

(6) leading us to speculate that "untapped" loading of a C-terminal signal peptide fragment makes use of other chaperones, such as TAPBP.

We considered it important to try to link findings in relation to mechanisms of β-cell antigen presentation obtained *in vitro* with the tissue inflammatory process taking place in subjects with type 1 diabetes. Our analysis shows that TAP expression is significantly increased in insulin-containing islets and correlated in its hyper-expression with HLA class I molecule expression. It has become a much vaunted metaphor that the β-cell contributes to its own destruction in various ways. In the particular setting of PPI presentation to cytotoxic T cells, it would appear that hyper-expression of TAP is a further example, certainly for HLA alleles such as HLA-A2402. In this way it may complement the effects of hyper-expression of HLA class I and hyper-glycaemic conditions (which upregulate PPI presentation (6)) in enhancing β-cell cytotoxicity under the inflammatory milieu that prevails in the islets of Langerhans in patients with type 1 diabetes.

Table 1. Preproinsulin epitopes identified by elution from specific HLA class I molecules.

Allele	Risk/Protection	PPI Signal Peptide	Other PPI regions
*HLA-A*0201*	Risk/neutral	**PPI15-24 (ALWGPDPAAA)**	No peptides found
*HLA-A*2402*	Risk	**PPI3-11 (LWMRLLPLL)**	No peptides found
*HLA-B*1801*	Risk	No peptides found	No peptides found
*HLA-B*3906*	Risk	**PPI5-12 (MRLLPLLA)**	No peptides found
*HLA-A*1101*	Protection	No peptides found	**PPI80-88 (LALEGSLQK)**
*HLA-B*3801*	Protection	**PPI5-14 (MRLLPLLALL)**	**PPI33-41 (SHLVEALYL)**

Figure Legends

Figure 1: PPI epitope discovery in HLA-B3906. (A) Tandem mass spectrometry analysis of collision-induced dissociation revealing the tandem mass spectrum of a peptide of mass 463.8 m/z and sequence MRLLPLLA. The correct identity of the peptide was proven by tandem mass spectrometry of the synthetic compound. (B) The table lists the amino acid sequence of the peptide with the expected b- and y-fragment ions (fragment ions extending from the amino- and carboxyl terminus respectively). Observed fragment ions are underlined. Tandem mass spectra and table of b- and y-fragment ions for PPI epitopes discovered in HLA-A1101 and B3801 are provided in **Supplementary Figure 2**. (C) Diagram indicates position of the PPI signal peptide in the ER membrane during co-translational translocation, and the sequences and positions of the signal peptides identified by elution of the naturally processed and presented immunopeptidome for different HLA molecules.

Figure 2: Processing of PPI signal peptide by SPP in a cell-free translocation assay. (A) *In vitro* translation of wild type (wt) PPI mRNA in the absence (lane 1) or presence of ER-derived microsomes (lanes 2 and 3) and SPP inhibitor $(Z\text{-}LL)_2$-ketone (lane 3). Microsomes containing radiolabelled translocated proinsulin and membrane integral signal peptides (SP) were isolated and analysed by SDS-PAGE and audioradiography. Lane 4, *in vitro*-translated reference peptide comprising the PPI signal sequence. Upon ER targeting and signal peptidase cleavage, liberated SP is released from the membrane fraction (lane 2) in a process that can be blocked in the presence of $(Z\text{-}LL)_2$-ketone inhibitor (lane 3) indicating SPP-catalysed cleavage. (B) *In vitro* translation of mutant PPI mRNA (P9L, A12L, A15L) under similar conditions shows cleavage-deficient SP that is retained in the membrane fraction irrespective of $(Z\text{-}LL)_2$-ketone inhibitor. (C) P9L, A12L, A15L SP mutant sequence. (D) Quantification of PPI signal peptide processing (mean, wt n=5, mutations n=2). Means

indicate the relative amounts of signal peptide obtained in lane 2 compared to the corresponding lane 3, where SPP was inhibited. Processing was quantified by comparing intensity of signal peptide in the absence (DMSO) and presence of SPP inhibitor $(Z\text{-}LL)_2$-ketone for each condition, given by the formula 100-(100x/y) where x is the intensity of the test band and y is the intensity of the band in the presence of full inhibition with $(Z\text{-}LL)_2$-ketone). Equal translocation efficiency was controlled by comparing the amount of proinsulin between conditions. **Supplementary Table 1** and **Supplementary Figure 3** for details.

Figure 3: Impact of signal peptide peptidase (SPP) knockout in PPI- expressing cells on HLA presentation of signal peptide-derived epitope presentation. The $PPI_{15\text{-}24}$ specific HLA-A0201 restricted T cell clone was cultured at 2:1 target to effector ratio with different cell lines representing K562-A2-PPI (positive control; presents $PPI_{15\text{-}24}$ in HLA-A0201); K562-A2 (negative control; lacks PPI) K562-A2-PPI-SPPmock (negative controls; 2 lines of mock CRISPR-Cas9 manipulation, see Methods) and K562-A2-PPI-SPPko (test conditions; 3 independent lines of CRISPR-Cas9 knockout of SPP). SPPko markedly reduces activation of the T cell clone, as shown by (A) the lower median fluorescence intensity of CD107a and (B) reduced percentage expression of CD107a. Bars and error bars represent mean ± SEM for 4 independently performed experiments.

Figure 4: Impact of siRNA knockdown of TAP and ERAP1 on epitope presentation. (A) Percentage mRNA knockdown in K562-A24-PPI cells treated with siRNA knockdown for *β2M*, *TAP1*, and *TAP2* genes and (B) *ERAP1* and *ERAP2 genes* (left panels) and resulting effect on MIP-1β production by the HLA-A2402-restricted $PPI_{3\text{-}11}$ specific CD8 T cell clone 4C6 upon co-culture with the different cells lines (right panels). Scrambled siRNAs are used

as control. ΔCt values of targeted knockdown were compared to ΔCt of scrambled siRNA, and expressed as the relative mRNA level of specific gene knockdown. Efficiency of relevant mRNA knockdown is high resulting in reduced PPI_{3-11} presentation for TAP1, TAP2 and ERAP1, but not ERAP2. B2M serves as a positive control. Bars/error bars represent mean ± SEM of technical duplicates from three independent experiments for mRNA knockdown and one representative example of MIP-1β production (two further repeats in **Supplementary Figure 9**).

Figure 5: Expression of TAP and ERAP1 in human pancreas. Pancreas samples from 6 control individuals and 6 patients with type 1 diabetes (**Supplementary Table 2**) were stained for TAP1, HLA-ABC and insulin. (A) Images are representative (same microscope and camera settings) of 18 islets from control cases, plus 18 insulin-deficient islets (IDI) and 18 insulin-containing (ICI) islets from patients with type 1 diabetes. The mean fluorescence intensity (MFI) for each antigen was determined within all imaged islets. The analysis reveals (B) a significant increase in TAP1 expression in ICIs from individuals with type 1 diabetes compared with IDIs or control islets. (C) Consistent with previous reports, a similar change was seen with HLA-ABC expression. (D) Comparing TAP1 and HLA-ABC expression within the same islets shows a positive correlation. Error bars represent mean values ± SEM, with a one-way ANOVA and a subsequent post-hoc Tukey's multiple comparison test used to determine significance between groups (***$p<0.001$).

Figure 6: Processing of PPI signal peptide. Model of PPI signal peptide processing in which N-terminal peptides may be released into the cytoplasm by SPP where they depend on TAP transport into the ER and ERAP1 trimming before loading into nascent HLA (illustrated

by example of PPI_{3-11} loading into HLA-A2402), in contrast ER luminal peptides are directly released into the ER lumen, not requiring TAP transport but equally requiring trimming by ERAP1 for optimal presentation (illustrated by example of PPI_{15-24} loading into HLA-A0201).

Acknowledgments

The authors are grateful to Professor John Todd (University of Oxford) for provision of the typed HLA class I cell lines and Dr Pierre Vantourout, King's College London for providing the pLG2C vector. This study was supported by the NIHR Biomedical Research Centre at Guy's and St Thomas' Hospital Trusts and King's College London, a Centre Grant from the Juvenile Diabetes Research Foundation (JDRF; 1-2007-1803 to MP), a JDRF Career Development Award to SJR (5-CDA-2014-221-A-N), a project grant 15/0005156 from Diabetes UK (to NGM & SJR) and a project grant FOR2290-TP1 from the Deutsche Forschungsgemeinschaft (to MKL).

No potential conflicts of interest relevant to this article were reported.

D.K-V. and M.E. designed and performed experiments, analysed data, conceived ideas, oversaw research, and wrote the manuscript. M.A.R., A.d.R., B.H., and N.Y. performed experiments. P.A.v.V., S.J.R, N.G.M., M.K.L. and M.P. conceived ideas, oversaw research, and wrote the manuscript. M.P. is the guarantor of this work and, as such, had full access to all the data in the study and takes responsibility for the integrity of the data and the accuracy of the data analysis.

References

1. Atkinson MA: The pathogenesis and natural history of type 1 diabetes. Cold Spring Harb Perspect Med 2012;2
2. DiLorenzo TP, Serreze DV: The good turned ugly: immunopathogenic basis for diabetogenic CD8+ T cells in NOD mice. Immunol Rev 2005;204:250-263
3. Nejentsev S, Howson JM, Walker NM, Szeszko J, Field SF, Stevens HE, Reynolds P, Hardy M, King E, Masters J, Hulme J, Maier LM, Smyth D, Bailey R, Cooper JD, Ribas G, Campbell RD, Clayton DG, Todd JA, Wellcome Trust Case Control C: Localization of type 1 diabetes susceptibility to the MHC class I genes HLA-B and HLA-A. Nature 2007;450:887-892
4. Kronenberg D, Knight RR, Estorninho M, Ellis RJ, Kester MG, de Ru A, Eichmann M, Huang GC, Powrie J, Dayan CM, Skowera A, van Veelen PA, Peakman M: Circulating preproinsulin signal peptide-specific CD8 T cells restricted by the susceptibility molecule HLA-A24 are expanded at onset of type 1 diabetes and kill beta-cells. Diabetes 2012;61:1752-1759
5. Luce S, Lemonnier F, Briand JP, Coste J, Lahlou N, Muller S, Larger E, Rocha B, Mallone R, Boitard C: Single insulin-specific CD8+ T cells show characteristic gene expression profiles in human type 1 diabetes. Diabetes 2011;60:3289-3299
6. Skowera A, Ellis RJ, Varela-Calvino R, Arif S, Huang GC, Van-Krinks C, Zaremba A, Rackham C, Allen JS, Tree TI, Zhao M, Dayan CM, Sewell AK, Unger WW, Drijfhout JW, Ossendorp F, Roep BO, Peakman M: CTLs are targeted to kill beta cells in patients with type 1 diabetes through recognition of a glucose-regulated preproinsulin epitope. J Clin Invest 2008;118:3390-3402
7. Willcox A, Richardson SJ, Bone AJ, Foulis AK, Morgan NG: Analysis of islet inflammation in human type 1 diabetes. Clin Exp Immunol 2009;155:173-181
8. Coppieters KT, Dotta F, Amirian N, Campbell PD, Kay TW, Atkinson MA, Roep BO, von Herrath MG: Demonstration of islet-autoreactive CD8 T cells in insulitic lesions from recent onset and long-term type 1 diabetes patients. J Exp Med 2012;209:51-60
9. Richardson SJ, Rodriguez-Calvo T, Gerling IC, Mathews CE, Kaddis JS, Russell MA, Zeissler M, Leete P, Krogvold L, Dahl-Jorgensen K, von Herrath M, Pugliese A, Atkinson MA, Morgan NG: Islet cell hyperexpression of HLA class I antigens: a defining feature in type 1 diabetes. Diabetologia 2016;59:2448-2458
10. Rigby MR, DiMeglio LA, Rendell MS, Felner EI, Dostou JM, Gitelman SE, Patel CM, Griffin KJ, Tsalikian E, Gottlieb PA, Greenbaum CJ, Sherry NA, Moore WV, Monzavi R, Willi SM, Raskin P, Moran A, Russell WE, Pinckney A, Keyes-Elstein L, Howell M, Aggarwal S, Lim N, Phippard D, Nepom GT, McNamara J, Ehlers MR, Team TDS: Targeting of memory T cells with alefacept in new-onset type 1 diabetes (T1DAL study): 12 month results of a randomised, double-blind, placebo-controlled phase 2 trial. Lancet Diabetes Endocrinol 2013;1:284-294
11. Howson JM, Walker NM, Clayton D, Todd JA, Type 1 Diabetes Genetics C: Confirmation of HLA class II independent type 1 diabetes associations in the major histocompatibility complex including HLA-B and HLA-A. Diabetes Obes Metab 2009;11 Suppl 1:31-45
12. Valdes AM, Erlich HA, Noble JA: Human leukocyte antigen class I B and C loci contribute to Type 1 Diabetes (T1D) susceptibility and age at T1D onset. Hum Immunol 2005;66:301-313
13. Townsend A, Bastin J, Gould K, Brownlee G, Andrew M, Coupar B, Boyle D, Chan S, Smith G: Defective presentation to class I-restricted cytotoxic T lymphocytes in vaccinia-infected cells is overcome by enhanced degradation of antigen. J Exp Med 1988;168:1211-1224
14. Chang SC, Momburg F, Bhutani N, Goldberg AL: The ER aminopeptidase, ERAP1, trims precursors to lengths of MHC class I peptides by a "molecular ruler" mechanism. Proc Natl Acad Sci U S A 2005;102:17107-17112
15. Spies T, Bresnahan M, Bahram S, Arnold D, Blanck G, Mellins E, Pious D, DeMars R: A gene in the human major histocompatibility complex class II region controlling the class I antigen presentation pathway. Nature 1990;348:744-747

16. Cresswell P: Intracellular surveillance: controlling the assembly of MHC class I-peptide complexes. Traffic 2000;1:301-305
17. Saric T, Chang SC, Hattori A, York IA, Markant S, Rock KL, Tsujimoto M, Goldberg AL: An IFN-gamma-induced aminopeptidase in the ER, ERAP1, trims precursors to MHC class I-presented peptides. Nat Immunol 2002;3:1169-1176
18. Neefjes J, Jongsma ML, Paul P, Bakke O: Towards a systems understanding of MHC class I and MHC class II antigen presentation. Nature reviews Immunology 2011;11:823-836
19. Martoglio B, Dobberstein B: Signal sequences: more than just greasy peptides. Trends Cell Biol 1998;8:410-415
20. Weihofen A, Binns K, Lemberg MK, Ashman K, Martoglio B: Identification of signal peptide peptidase, a presenilin-type aspartic protease. Science 2002;296:2215-2218
21. Lemberg MK, Martoglio B: Requirements for signal peptide peptidase-catalyzed intramembrane proteolysis. Molecular cell 2002;10:735-744
22. Lemberg MK, Bland FA, Weihofen A, Braud VM, Martoglio B: Intramembrane proteolysis of signal peptides: an essential step in the generation of HLA-E epitopes. J Immunol 2001;167:6441-6446
23. Wei ML, Cresswell P: HLA-A2 molecules in an antigen-processing mutant cell contain signal sequence-derived peptides. Nature 1992;356:443-446
24. Henderson RA, Michel H, Sakaguchi K, Shabanowitz J, Appella E, Hunt DF, Engelhard VH: HLA-A2.1-associated peptides from a mutant cell line: a second pathway of antigen presentation. Science 1992;255:1264-1266
25. El Hage F, Stroobant V, Vergnon I, Baurain JF, Echchakir H, Lazar V, Chouaib S, Coulie PG, Mami-Chouaib F: Preprocalcitonin signal peptide generates a cytotoxic T lymphocyte-defined tumor epitope processed by a proteasome-independent pathway. Proc Natl Acad Sci U S A 2008;105:10119-10124
26. Bland FA, Lemberg MK, McMichael AJ, Martoglio B, Braud VM: Requirement of the proteasome for the trimming of signal peptide-derived epitopes presented by the nonclassical major histocompatibility complex class I molecule HLA-E. J Biol Chem 2003;278:33747-33752
27. Meiring HD, van der Heeft E, ten Hove GJ, de Jong APJM: Nanoscale LC–MS(n): technical design and applications to peptide and protein analysis. Journal of Separation Science 2002;25:557-568
28. Stepniak D, Wiesner M, de Ru AH, Moustakas AK, Drijfhout JW, Papadopoulos GK, van Veelen PA, Koning F: Large-scale characterization of natural ligands explains the unique gluten-binding properties of HLA-DQ2. J Immunol 2008;180:3268-3278
29. Knight RR, Kronenberg D, Zhao M, Huang GC, Eichmann M, Bulek A, Wooldridge L, Cole DK, Sewell AK, Peakman M, Skowera A: Human beta-cell killing by autoreactive preproinsulin-specific CD8 T cells is predominantly granule-mediated with the potency dependent upon T-cell receptor avidity. Diabetes 2013;62:205-213
30. Nilsson IM, von Heijne G: Determination of the distance between the oligosaccharyltransferase active site and the endoplasmic reticulum membrane. J Biol Chem 1993;268:5798-5801
31. Martoglio B, Hauser S, Dobberstein B: Cotranslational translocation of proteins into microsomes derived from the rough endoplasmic reticulum of mammalian cells. In *Cell Biology: A Laboratory Handbook* Celis JE, Ed. San Diego, CA, Academic Press, 1998, p. 265–274
32. Weihofen A, Lemberg MK, Ploegh HL, Bogyo M, Martoglio B: Release of signal peptide fragments into the cytosol requires cleavage in the transmembrane region by a protease activity that is specifically blocked by a novel cysteine protease inhibitor. J Biol Chem 2000;275:30951-30956
33. Wiltfang J, Smirnov A, Schnierstein B, Kelemen G, Matthies U, Klafki HW, Staufenbiel M, Huther G, Ruther E, Kornhuber J: Improved electrophoretic separation and immunoblotting of beta-amyloid (A beta) peptides 1-40, 1-42, and 1-43. Electrophoresis 1997;18:527-532
34. Lemberg MK, Martoglio B: Analysis of polypeptides by sodium dodecyl sulfate-polyacrylamide gel electrophoresis alongside in vitro-generated reference peptides. Anal Biochem 2003;319:327-331

35. Eichmann M, de Ru A, van Veelen PA, Peakman M, Kronenberg-Versteeg D: Identification and characterisation of peptide binding motifs of six autoimmune disease-associated human leukocyte antigen-class I molecules including HLA-B*39:06. Tissue antigens 2014;84:378-388
36. Kovjazin R, Volovitz I, Daon Y, Vider-Shalit T, Azran R, Tsaban L, Carmon L, Louzoun Y: Signal peptides and trans-membrane regions are broadly immunogenic and have high CD8+ T cell epitope densities: Implications for vaccine development. Mol Immunol 2011;48:1009-1018
37. Voss M, Schroder B, Fluhrer R: Mechanism, specificity, and physiology of signal peptide peptidase (SPP) and SPP-like proteases. Biochim Biophys Acta 2013;1828:2828-2839
38. Li SC, Deber CM: A measure of helical propensity for amino acids in membrane environments. Nat Struct Biol 1994;1:368-373
39. Anderson KS, Zeng W, Sasada T, Choi J, Riemer AB, Su M, Drakoulakos D, Kang YJ, Brusic V, Wu C, Reinherz EL: Impaired tumor antigen processing by immunoproteasome-expressing CD40-activated B cells and dendritic cells. Cancer immunology, immunotherapy : CII 2011;60:857-867
40. Lundh M, Bugliani M, Dahlby T, Chou DH, Wagner B, Ghiasi SM, De Tata V, Chen Z, Lund MN, Davies MJ, Marchetti P, Mandrup-Poulsen T: The immunoproteasome is induced by cytokines and regulates apoptosis in human islets. The Journal of endocrinology 2017;233:369-379
41. Baschal EE, Baker PR, Eyring KR, Siebert JC, Jasinski JM, Eisenbarth GS: The HLA-B 3906 allele imparts a high risk of diabetes only on specific HLA-DR/DQ haplotypes. Diabetologia 2011;54:1702-1709
42. Avci D, Lemberg MK: Clipping or Extracting: Two Ways to Membrane Protein Degradation. Trends Cell Biol 2015;25:611-622
43. Panagiotopoulos C, Qin H, Tan R, Verchere CB: Identification of a beta-cell-specific HLA class I restricted epitope in type 1 diabetes. Diabetes 2003;52:2647-2651
44. Ouyang Q, Standifer NE, Qin H, Gottlieb P, Verchere CB, Nepom GT, Tan R, Panagiotopoulos C: Recognition of HLA class I-restricted beta-cell epitopes in type 1 diabetes. Diabetes 2006;55:3068-3074
45. Johnson AE, van Waes MA: The translocon: a dynamic gateway at the ER membrane. Annu Rev Cell Dev Biol 1999;15:799-842
46. Rapoport TA, Rolls MM, Jungnickel B: Approaching the mechanism of protein transport across the ER membrane. Curr Opin Cell Biol 1996;8:499-504
47. Dalbey RE, Lively MO, Bron S, van Dijl JM: The chemistry and enzymology of the type I signal peptidases. Protein Sci 1997;6:1129-1138
48. Fluhrer R, Martin L, Klier B, Haug-Kroper M, Grammer G, Nuscher B, Haass C: The alpha-helical content of the transmembrane domain of the British dementia protein-2 (Bri2) determines its processing by signal peptide peptidase-like 2b (SPPL2b). J Biol Chem 2012;287:5156-5163
49. Lemberg MK, Martoglio B: On the mechanism of SPP-catalysed intramembrane proteolysis; conformational control of peptide bond hydrolysis in the plane of the membrane. FEBS Lett 2004;564:213-218

Figure 1

A

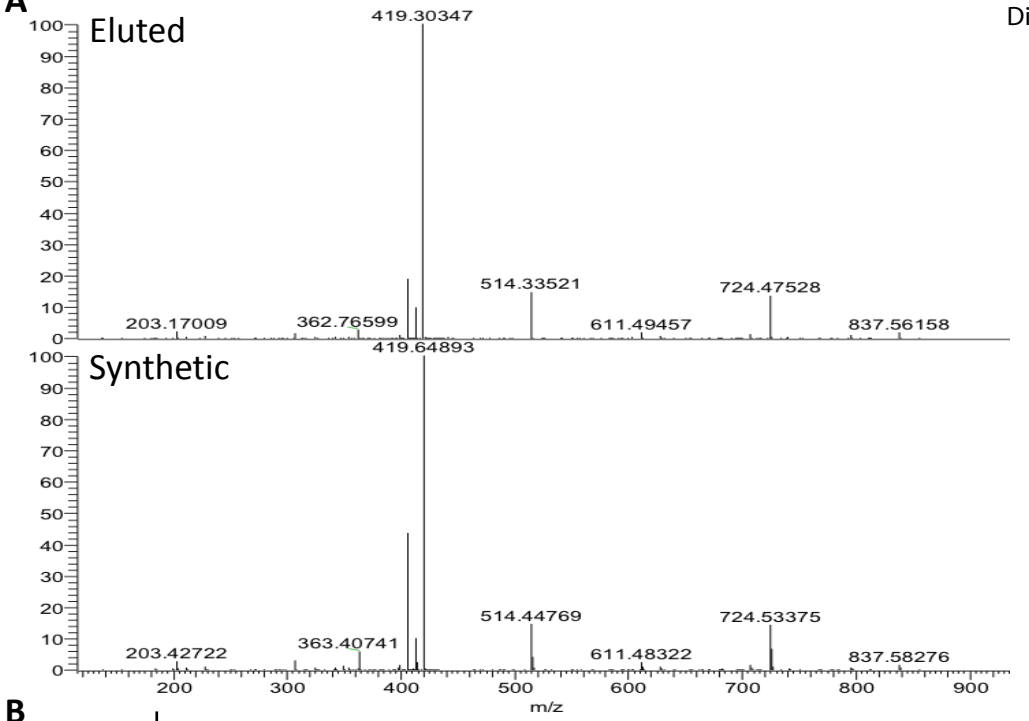

B

b_n ions	132.0	288.1	401.2	514.3	611.4	724.5	837.5	908.6
Peptide	M	R	L	L	P	L	L	A
y_n ions	951.7	795.6	639.4	526.4	413.3	316.2	203.1	90.1

C

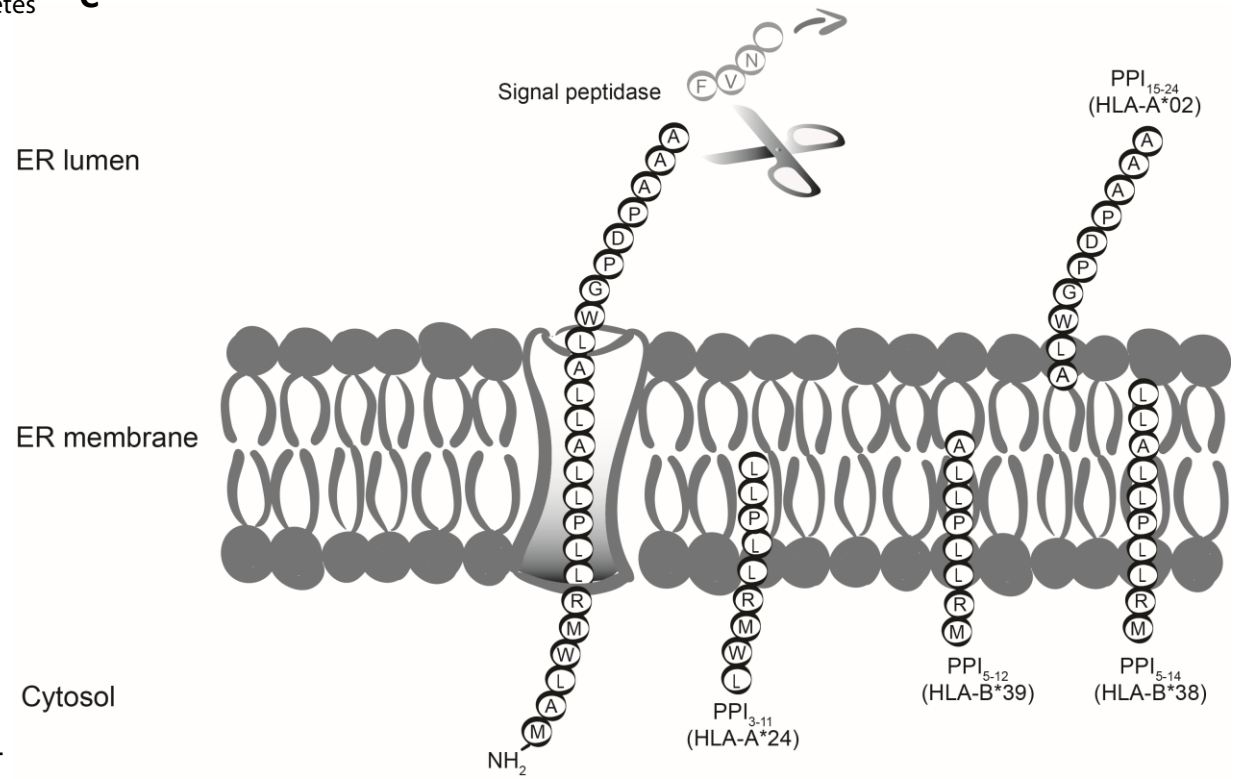

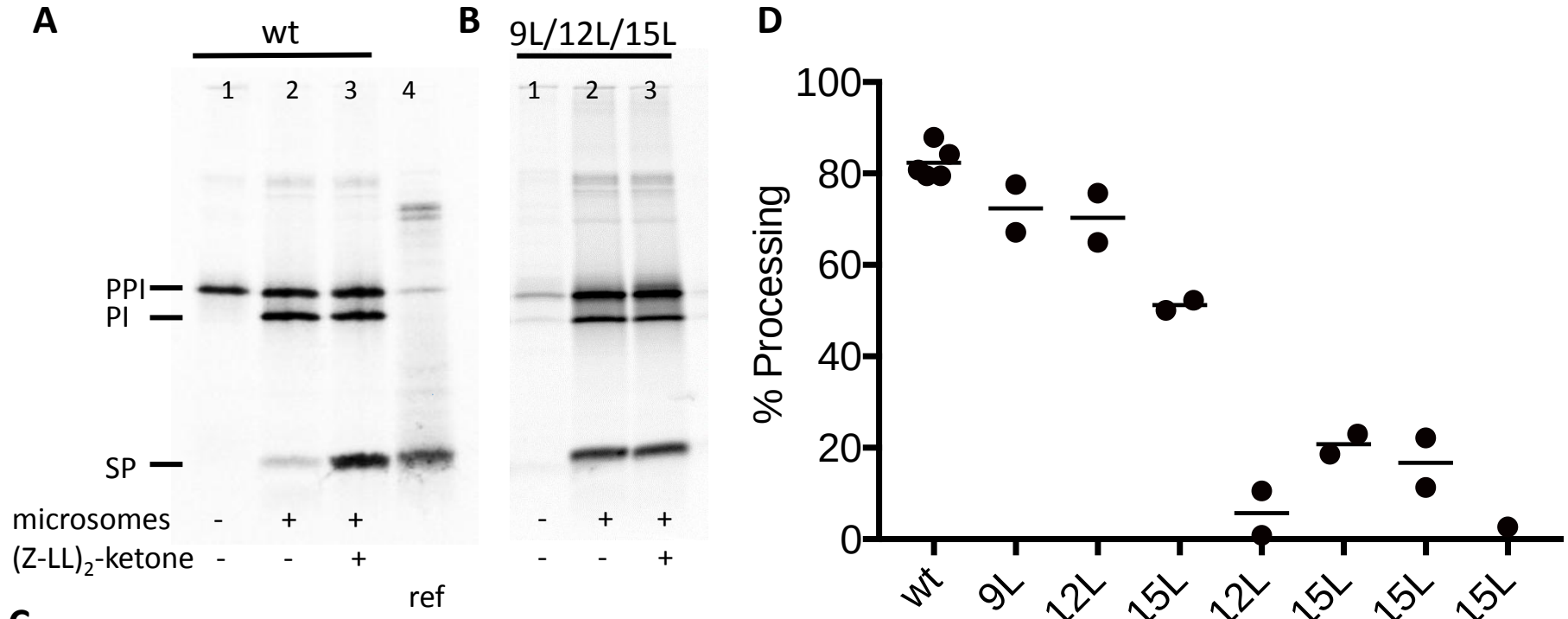

C

Wild type: MALWMRLLPLLALLALWGPDPAAA

Triple mutant: MALWMRLLLLLLLLLLWGPDPAAA

Figure 3

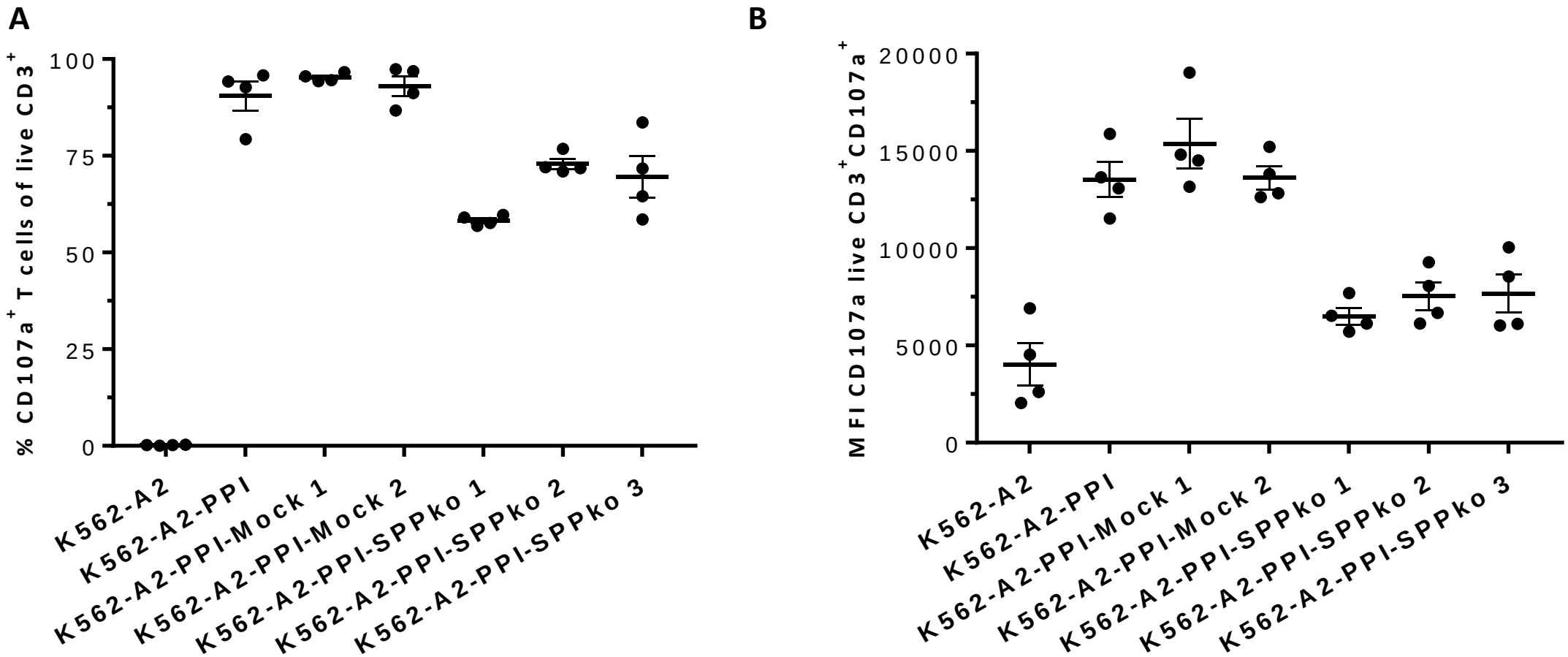
A
% CD107a+ T cells of live CD3+
100
75
50
25
0
K562-A2
K562-A2-PPI
K562-A2-PPI-Mock 1
K562-A2-PPI-Mock 2
K562-A2-PPI-SPPko 1
K562-A2-PPI-SPPko 2
K562-A2-PPI-SPPko 3
B
MFI CD107a live CD3+CD107a+
20000
15000
10000
5000
0
K562-A2
K562-A2-PPI
K562-A2-PPI-Mock 1
K562-A2-PPI-Mock 2
K562-A2-PPI-SPPko 1
K562-A2-PPI-SPPko 2
K562-A2-PPI-SPPko 3

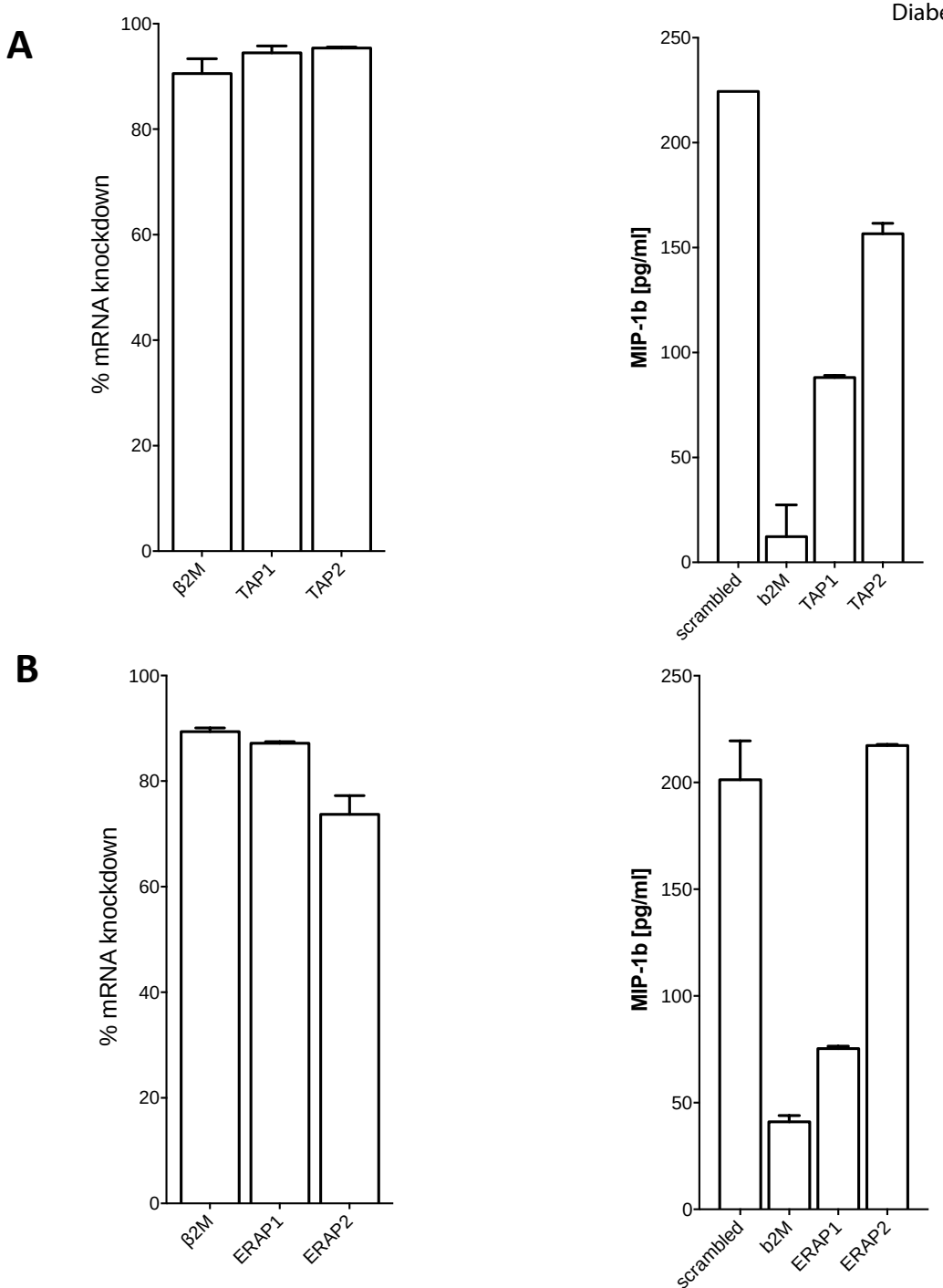
A
% mRNA knockdown
100
80
60
40
20
0
β2M
TAP1
TAP2
MIP-1b [pg/ml]
250
200
150
100
50
0
scrambled
b2M
TAP1
TAP2
B
% mRNA knockdown
100
80
60
40
20
0
β2M
ERAP1
ERAP2
MIP-1b [pg/ml]
250
200
150
100
50
0
scrambled
b2M
ERAP1
ERAP2

Figure 5

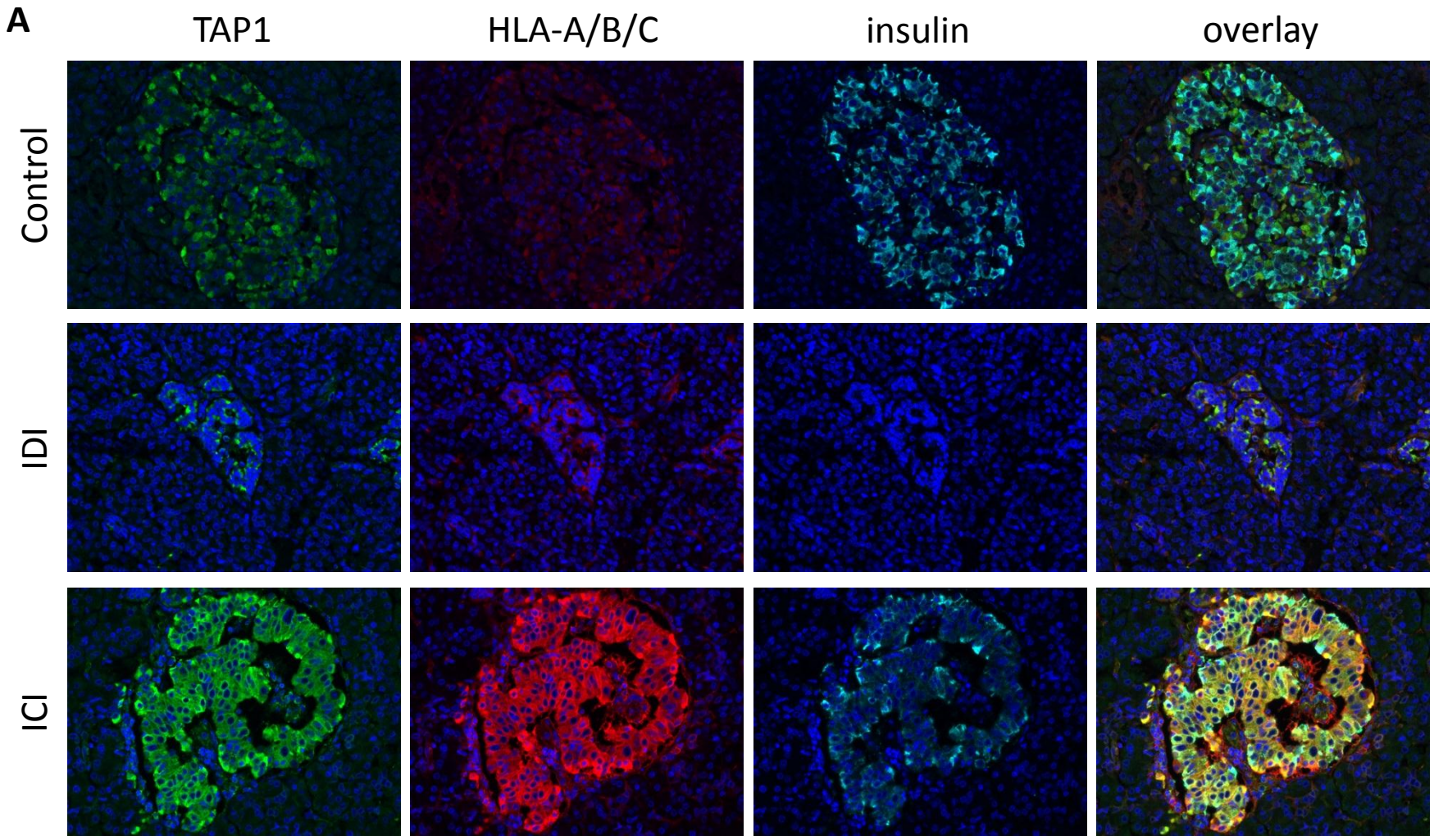
A
TAP1
HLA-A/B/C
insulin
overlay
Control
IDI
ICI

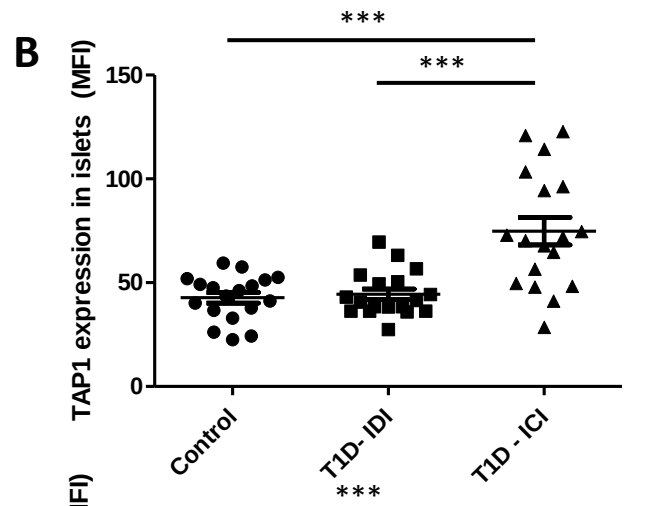
B
***
***
TAP1 expression in islets (MFI)
150
100
50
0
Control
T1D- IDI
T1D - ICI

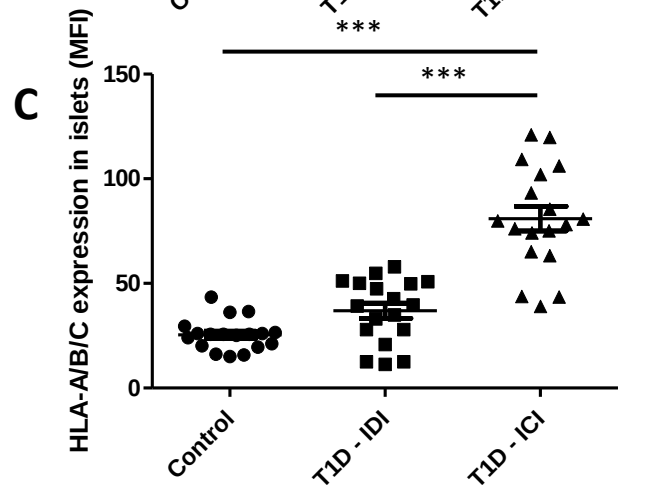
C
***
***
HLA-A/B/C expression in islets (MFI)
150
100
50
0
Control
T1D - IDI
T1D - ICI

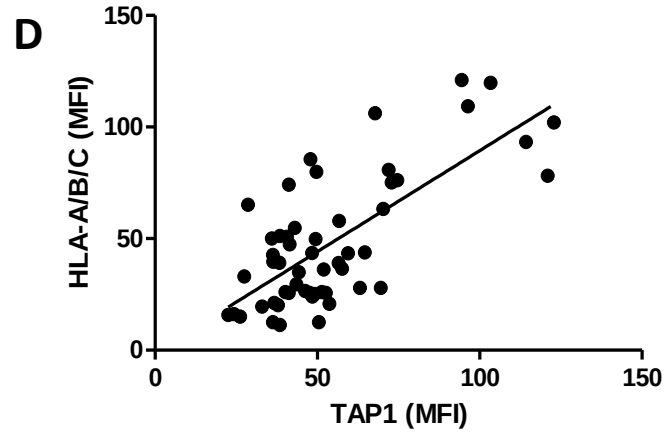
D
HLA-A/B/C (MFI)
150
100
50
0
0
50
100
150
TAP1 (MFI)

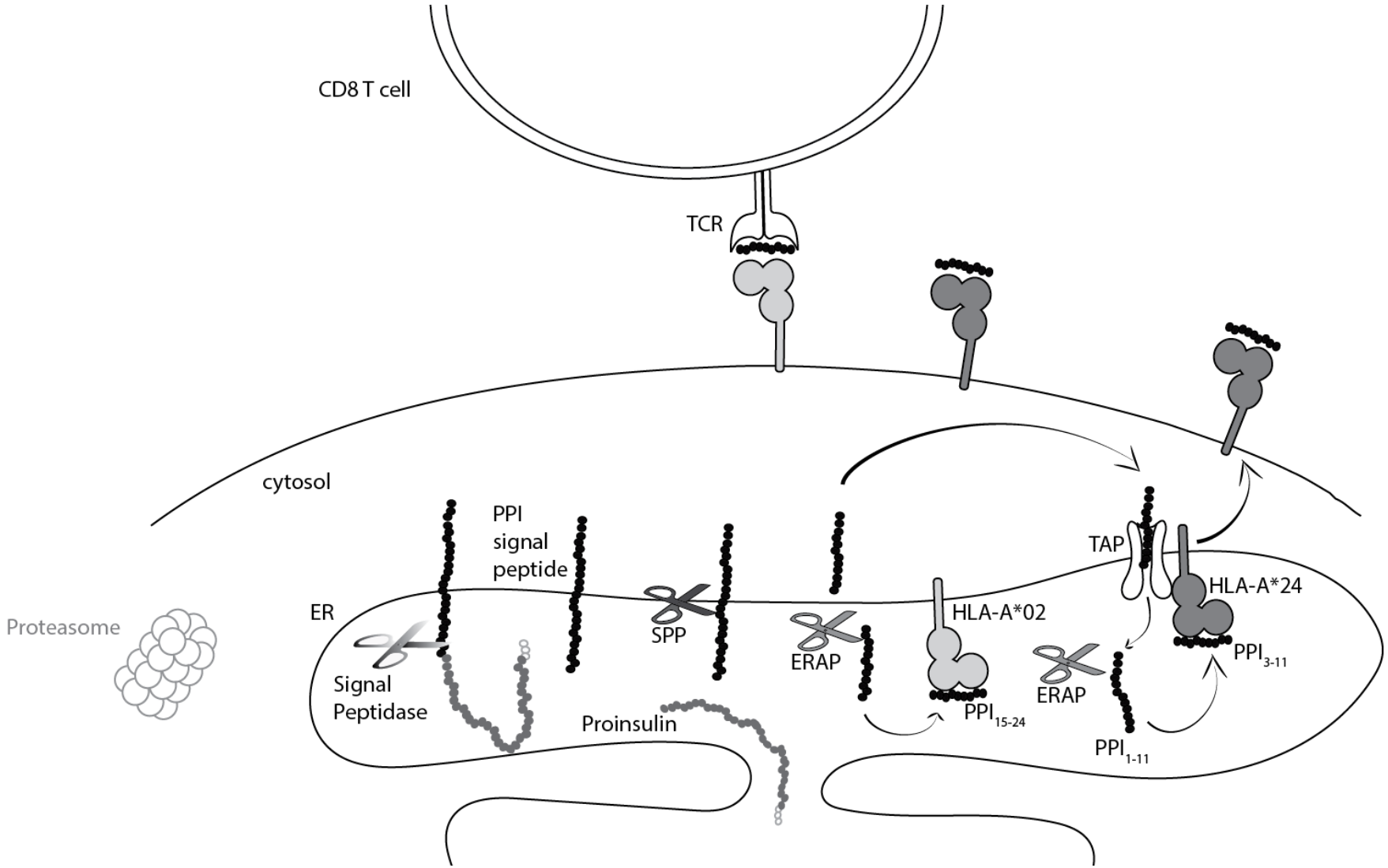
CD8 T cell
TCR
cytosol
PPI
signal
peptide
ER
Proteasome
Signal
Peptidase
SPP
ERAP
HLA-A*02
TAP
HLA-A*24
PPI3-11
ERAP
PPI15-24
PPI1-11
Proinsulin

Supplementary Table 1: Site directed mutation of signal peptide of preproinsulin

Designation	Sequence
Wild type PPI SP sequence	MALWMRLLPLLALLALWGPDPAAA
9L mutant	MALWMRLLLLLLLLLWGPDPAAA
12L mutant	MALWMRLLLLLLLLLWGPDPAAA
15L mutant	MALWMRLLLLLLLLLWGPDPAAA
9L/12L mutant	MALWMRLLLLLLLLLWGPDPAAA
9L/15L mutant	MALWMRLLLLLLLLLWGPDPAAA
12L/15L mutant	MALWMRLLLLLLLLLWGPDPAAA
9L/12L/15L mutant	MALWMRLLLLLLLLLWGPDPAAA

Supplementary Table 2: Details of subjects studied for pancreatic expression of antigen processing enzymes

Case ID	Group	Source	Donor Status	Age (years)	Duration
485 88	No diabetes control	UK Pancreas Biobank	Autopsy	2	
315 89	No diabetes control	UK Pancreas Biobank	Autopsy	9	
65 71	No diabetes control	UK Pancreas Biobank	Autopsy	40	
8579	No diabetes control	UK Pancreas Biobank	Autopsy	7	
540 91	No diabetes control	UK Pancreas Biobank	Autopsy	11	
PAN8	No diabetes control	UK Pancreas Biobank	Autopsy	19	
E560	Type 1 diabetes	UK Type 1 diabetes Biobank	Organ Donor	42	1.5y
Sc115	Type 1 diabetes	UK Type 1 diabetes Biobank	Autopsy	1	0 ‘Recent’
E124B	Type 1 diabetes	UK Type 1 diabetes Biobank	Autopsy	17	0 ‘Recent’
E375	Type 1 diabetes	UK Type 1 diabetes Biobank	Autopsy	11	unknown
11746	Type 1 diabetes	UK Type 1 diabetes Biobank	Autopsy	6	1 week
11713	Type 1 diabetes	UK Type 1 diabetes Biobank	Autopsy	3	3 months

Supplementary Table 3: Details of the staining protocol for each antibody employed in the current study.

Primary Antibody	Manufacturer and clone	Antigen Retrieval	Antibody Dilution	Incubation time with primary antibody	Secondary Detection System
HLA-ABC	Abcam C#ab70328 Mouse monoclonal EMR8-5	10mM citrate pH6.0	1/1000	1h at RT	Immunofluoroscence staining using anti-mouse IgG (H+L) Alexa Fluor™-conjugated secondary antibodies (1/400 for 1h)
Insulin	Dako C#A0564 Guinea-pig polyclonal	10mM citrate pH6.0	1/700	1h at RT	Immunofluoroscence staining using anti-guinea-pig IgG (H+L) Alexa Fluor™ -conjugated secondary antibodies (1/400 for 1h)
Glucagon	Abcam C#ab92517 Rabbit monoclonal EP3070	10mM citrate pH6.0	1/4000	1h at RT	Immunofluoroscence staining using anti-rabbit IgG (H+L) Alexa Fluor™-conjugated secondary antibodies (1/400 for 1h)
TAP1	Protein Tech C#11114-1-AP Rabbit polyclonal	10mM citrate pH6.0	1/200	o/n 4°C	Immunofluoroscence staining using anti-rabbit IgG (H+L) Alexa Fluor™ -conjugated secondary antibodies (1/400 for 1h)
ERAP	R & D Systems C#AF2334 Goat polyclonal	10mM Tris, 1mM EDTA pH9.0	1/200	o/n 4°C	Dako REAL™ Envision™ Detection System with anti-goat IgG HRP-conjugated secondary antibodies (1/800 for 1h).

Legend supplementary Table 3: **Details of the staining protocol for each antibody employed in the current study.** Where multiple antigens were stained on the same section, antibodies were applied sequentially (staining order: anti-TAP1 (overnight at 4°C) followed by anti-HLA-ABC (1h at room temperature) or anti-glucagon (1h at room temperature) then anti-insulin plus DAPI (1h at room temperature)).

Supplementary Table 4: Oligonucleotides used for CRISPR-mediated gene knockout.

	Forward	**Reverse**
Exon 2	GAAGCGGGCGGCATCCCGGCGTTTT	GCCGGGATGCCGCCCGCTTCCGGTG
Exon 3	GCAGGAGGTTGATGTACTCCGTTTT	GGAGTACATCAACCTCCTGCCGGTG
Exon 10	GCAGCCTACATCTTCGGCCTGTTTT	AGGCCGAAGATGTAGGCTGCCGGTG
Exon 11	CAGGACAGGAAAACCGATGCGTTTT	GCATCGGTTTTCCTGTCCTGCGGTG

Supplementary Table 5. Eluted epitopes are not selectively derived from SP containing source protein nor their signal peptide region.

	HLA-A*02:01	HLA-A*11:01	HLA-A*24:02	HLA-B*18:01	HLA-B*38:01	HLA-B*39:06	All HLA	Human proteome
Source proteins	**458**	**667**	**190**	**510**	**378**	**259**	**2462**	**20226**
Number of source proteins containing a signal peptide	**26**	**29**	**17**	**25**	**35**	**21**	**153**	**3560**
Frequency of signal peptide containing source proteins	**5.68%**	**4.35%**	**8.95%**	**4.90%**	**9.26%**	**8.11%**	**6.21%**	**17.6%**
Number of proteins with signal peptide-derived epitope	**12**	**2**	**4**	**5**	**4**	**13**	**40**	
Frequency of identified SP epitopes from SP-Protein	**46.15%**	**6.90%**	**23.53%**	**20.00%**	**11.43%**	**61.90%**	**26.14%**	

Source Proteins are those represented by at least one epitope with Mascot Score >40 within our HLA class I elution data (1). Uniprot (2) (access via http://www.uniprot.org/) retrieve/ID mapping function was used to identify signal peptide containing source proteins. SP, signal peptide.

Supplementary Table 6. Putative PPI epitopes identified by in silico binding prediction algorithms.

Binding prediction were performed by SYFPEITHI (3) (access via : www.syfpeithi.de)) to identify putative PPI epitopes to compare eluted epitopes to those identified in silico. Epitopes derived from the PPI signal peptide are highlighted in bold and those identified by elution in green.

	A2	9-mer	Score	A11	9-mer	Score	A24	9-mer	Score	B18	8-mer	Score	B38	9-mer	Score
1	6	**RLLPLLALL**	31	38	ALYLVCGER	18	6	**RLLPLLALL**	15	34	HLVEALYL	15	33	SHLVEALYL	21
2	2	**ALWMRLLPL**	28	81	ALEGSLQKR	18	17	**WGPDPAAAF**	13	36	VEALYLVC	14	5	**MRLLPLLAL**	18
3	34	HLVEALYLV	27	35	LVEALYLVC	16	39	LYLVCGERG	13	56	REAEDLQV	14	6	**RLLPLLALL**	14
4	60	DLQVGQVEL	25	75	GSLQPLALE	16	97	TSICSLYQL	13	61	LQVGQVEL	13	3	**LWMRLLPLL**	13
5	15	**ALWGPDPAA**	22	76	SLQPLALEG	16	3	**LWMRLLPLL**	12	32	GSHLVEAL	12	2	**ALWMRLLPL**	12
6	8	**LPLLALLAL**	20	32	GSHLVEALY	15	5	**MRLLPLLAL**	12	42	VCGERGFF	12	8	**LPLLALLAL**	12
7	3	**LWMRLLPLL**	19	80	LALEGSLQK	15	8	**LPLLALLAL**	12	58	AEDLQVGQ	12	31	CGSHLVEAL	12
8	5	**MRLLPLLAL**	19	62	QVGQVELGG	14	22	**AAAFVNQHL**	12	3	**LWMRLLPL**	11	60	DLQVGQVEL	12
9	81	ALEGSLQKR	19	84	GSLQKRGIV	14	31	CGSHLVEAL	12	6	**RLLPLLAL**	11	72	PGAGSLQPL	12
10	7	**LLPLLALLA**	18	85	SLQKRGIVE	14	33	SHLVEALYL	12	9	**PLLALLAL**	11	74	AGSLQPLAL	12
11	76	SLQPLALEG	18	96	CTSICSLYQ	14	49	FYTPKTRRE	12	33	SHLVEALY	11	97	TSICSLYQL	12
12	22	**AAAFVNQHL**	17	2	**ALWMRLLPL**	13	78	QPLALEGSL	12	41	LVCGERGF	11	28	QHLCGSHLV	11
13	69	GGGPGAGSL	17	4	**WMRLLPLLA**	13	2	**ALWMRLLPL**	11	44	GERGFFYT	11	69	GGGPGAGSL	11
14	97	TSICSLYQL	17	7	**LLPLLALLA**	13	53	KTRREAEDL	11	66	VELGGGPG	11	78	QPLALEGSL	11
15	9	**PLLALLALW**	16	47	GFFYTPKTR	13	69	GGGPGAGSL	11	75	GSLQPLAL	11	94	QCCTSICSL	11
16	10	**LLALLALWG**	16	10	**LLALLALWG**	12	74	AGSLQPLAL	11	82	LEGSLQKR	11	22	**AAAFVNQHL**	10
17	31	CGSHLVEAL	16	29	HLCGSHLVE	12	94	QCCTSICSL	11	92	VEQCCTSI	11	91	IVEQCCTSI	10
18	58	AEDLQVGQV	16	60	DLQVGQVEL	12	27	NQHLCGSHL	10	96	CTSICSLY	11	17	**WGPDPAAAF**	9
19	94	QCCTSICSL	16	98	SICSLYQLE	12	40	YLVCGERGF	10	1	**MALWMRLL**	10	27	NQHLCGSHL	9
20	12	**ALLALWGPD**	15	12	**ALLALWGPD**	11	41	LVCGERGFF	10	18	**GPDPAAAF**	10	41	LVCGERGFF	9
21	13	**LLALWGPDP**	15	41	LVCGERGFF	11	60	DLQVGQVEL	10	43	**CGERGFFY**	10	53	KTRREAEDL	9
22	18	**GPDPAAAFV**	15	45	ERGFFYTPK	11	72	PGAGSLQPL	10	54	TRREAEDL	10	83	EGSLQKRGI	9
23	28	QHLCGSHLV	15	50	YTPKTRREA	11	83	EGSLQKRGI	10	101	SLYQLENY	10	40	YLVCGERGF	8
24	33	SHLVEALYL	15	53	KTRREAEDL	11	91	IVEQCCTSI	10	4	**WMRLLPLL**	9	55	RREAEDLQV	8
25	38	ALYLVCGER	15	97	TSICSLYQL	11	102	LYQLENYCN	10	7	**LLPLLALL**	9	54	TRREAEDLQ	7

	A2	10-mer	Score	A11	10-mer	Score	A24	10-mer	Score	B18	9-mer	Score	B38	10-mer	Score
1	2	**ALWMRLLPLL**	28	79	PLALEGSLQK	21	39	LYLVCGERGF	22	100	CSLYQLENY	15	5	MRLLPLLALL	19
2	7	**LLPLLALLAL**	28	75	GSLQPLALEG	20	5	**MRLLPLLALL**	14	60	DLQVGQVEL	14	59	EDLQVGQVEL	14
3	4	**WMRLLPLLAL**	24	84	GSLQKRGIVE	19	26	VNQHLCGSHL	13	31	CGSHLVEAL	13	7	**LLPLLALLAL**	13
4	29	HLCGSHLVEA	24	32	GSHLVEALYL	18	1	**MALWMRLLPL**	12	44	GERGFFYTP	13	73	GAGSLQPLAL	13
5	15	**ALWGPDPAAA**	22	6	**RLLPLLALLA**	15	2	**ALWMRLLPLL**	12	56	REAEDLQVG	13	1	**MALWMRLLPL**	12
6	1	**MALWMRLLPL**	21	35	LVEALYLVCG	15	7	**LLPLLALLAL**	12	8	**LPLLALLAL**	12	2	**ALWMRLLPLL**	12
7	90	GIVEQCCTSI	21	85	SLQKRGIVEQ	15	30	LCGSHLVEAL	12	36	VEALYLVCG	12	4	**WMRLLPLLAL**	12
8	85	SLQKRGIVEQ	20	98	SICSLYQLEN	15	59	EDLQVGQVEL	12	58	AEDLQVGQV	12	32	GSHLVEALYL	12
9	6	**RLLPLLALLA**	19	44	**GERGFFYTPK**	14	77	LQPLALEGSL	12	74	AGSLQPLAL	12	33	SHLVEALYLV	12
10	10	**LLALLALWGP**	19	9	**PLLALLALWG**	13	90	GIVEQCCTSI	12	78	QPLALEGSL	12	68	LGGGPGAGSL	12
11	33	SHLVEALYLV	19	97	TSICSLYQLE	13	16	**LWGPDPAAAF**	11	82	LEGSLQKRG	12	93	EQCCTSICSL	12
12	76	SLQPLALEGS	19	29	HLCGSHLVEA	12	21	**PAAAFVNQHL**	11	3	**LWMRLLPLL**	11	26	VNQHLCGSHL	11
13	96	CTSICSLYQL	19	47	GFFYTPKTRR	12	49	FYTPKTRREA	11	5	**MRLLPLLAL**	11	28	QHLCGSHLVE	11
14	5	**MRLLPLLALL**	18	53	KTRREAEDLQ	12	52	PKTRREAEDL	11	6	**RLLPLLALL**	11	30	LCGSHLVEAL	11
15	13	**LLALWGPDPA**	18	2	**ALWMRLLPLL**	11	73	GAGSLQPLAL	11	32	GSHLVEALY	11	52	PKTRREAEDL	11
16	30	LCGSHLVEAL	17	12	**ALLALWGPDP**	11	93	EQCCTSICSL	11	42	VCGERGFFY	11	71	GPGAGSLQPL	11
17	73	GAGSLQPLAL	17	15	**ALWGPDPAAA**	11	40	YLVCGERGFF	10	95	CCTSICSLY	11	96	CTSICSLYQL	11
18	68	LGGGPGAGSL	16	34	HLVEALYLVC	11	68	LGGGPGAGSL	10	9	**PLLALLALW**	10	16	**LWGPDPAAAF**	10
19	80	LALEGSLQKR	16	41	LVCGERGFFY	11	71	GPGAGSLQPL	10	27	NQHLCGSHL	10	21	**PAAAFVNQHL**	10
20	12	**ALLALWGPDP**	15	100	CSLYQLENYC	11	82	LEGSLQKRGI	10	40	YLVCGERGF	10	77	LQPLALEGSL	10
21	57	EAEDLQVGQV	15	4	**WMRLLPLLAL**	10	96	CTSICSLYQL	10	41	LVCGERGFF	10	40	YLVCGERGFF	9
22	71	GPGAGSLQPL	15	7	**LLPLLALLAL**	10	4	**WMRLLPLLAL**	9	66	VELGGGPGA	10	54	TRREAEDLQV	9
23	14	**LALWGPDPAA**	14	25	FVNQHLCGSH	10	32	GSHLVEALYL	9	2	**ALWMRLLPL**	9	39	LYLVCGERGF	8
24	77	LQPLALEGSL	14	37	EALYLVCGER	10	24	**AFVNQHLCGS**	6	17	**WGPDPAAAF**	9	45	ERGFFYTPKT	8
25	101	SLYQLENYCN	14	46	RGFFYTPKTR	10	42	VCGERGFFYT	6	53	KTRREAEDL	9	55	RREAEDLQVG	8

Supplementary Figure 1

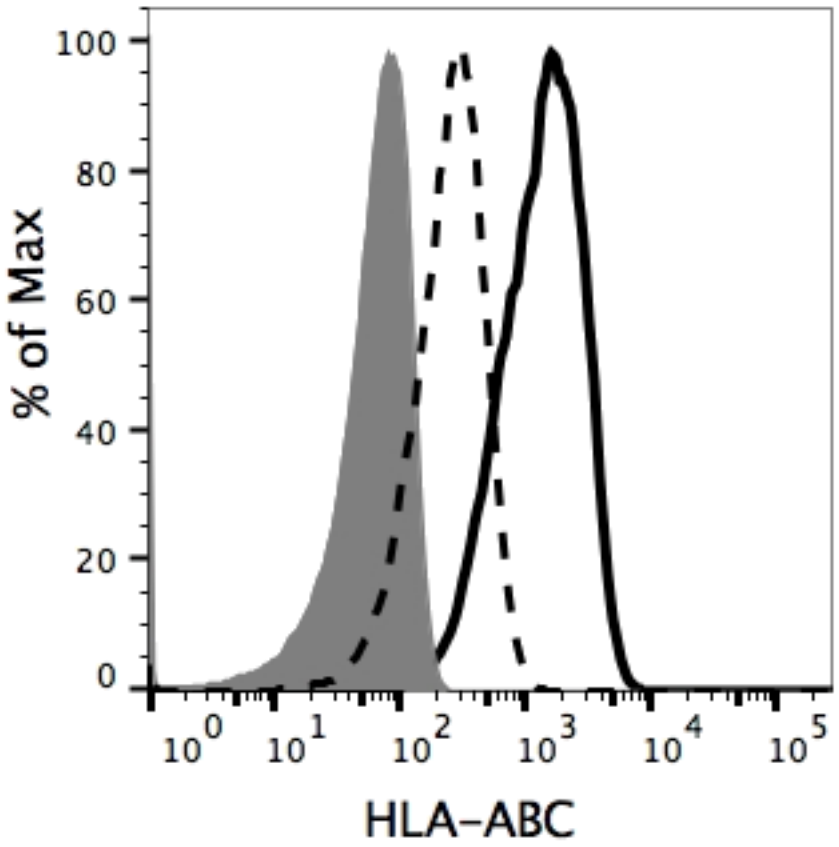

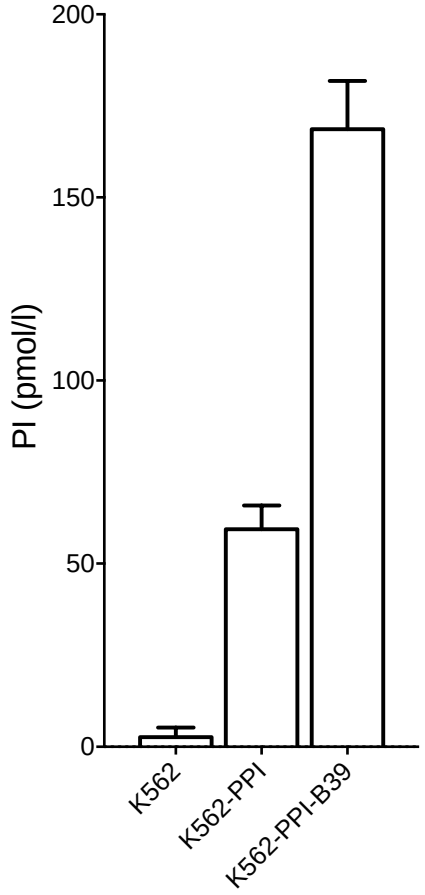

Legend Supplementary Figure 1: **Representative Expression of HLA class I and secretion of proinsulin.** Expression of HLA class I and secretion of proinsulin by the generated K562-PPI (dashed line) and K562-PPI-HLA (solid line) cell lines (isotype control grey shaded). Single cell cloning was performed to select for the K562-PPI-HLA cell line with best combination of HLA class I expression (left) and Proinsulin expression (right). Data is representative, with B*3906 shown, and similar data obtained for A*11:01, B*1801 and B*38:01.

Supplementary Figure 2 A) HLA-A*1101 Epitope PPI_{80-88}

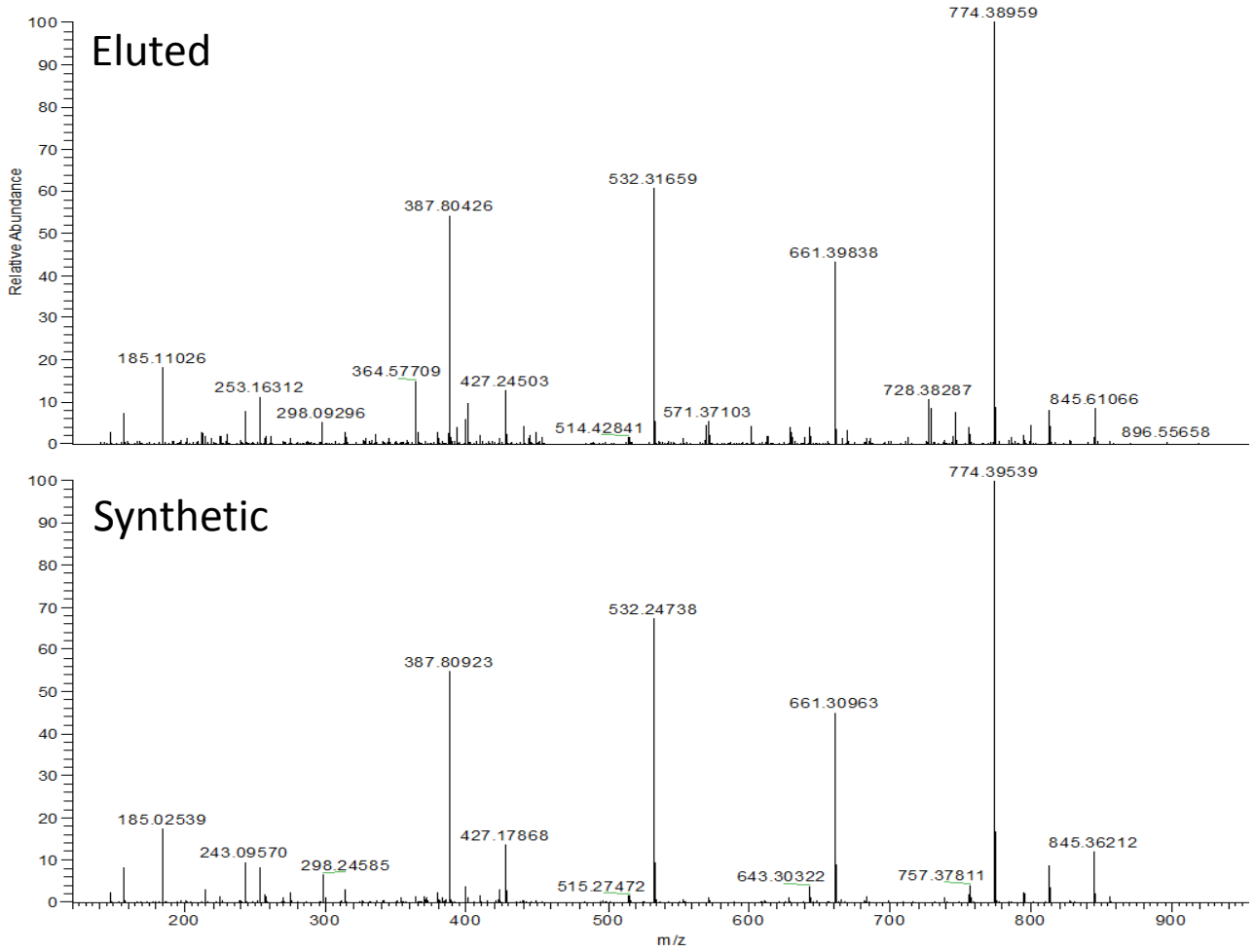

b_n ions	114.1	185.1	298.2	427.3	484.3	571.3	684.4	812.5	958.6
Peptide	L	A	L	E	G	S	L	Q	K
y_n ions	958.6	845.5	774.4	661.4	523.3	475.3	388.3	275.2	147.1

Supplementary Figure 2: PPI epitope discovery
Tandem mass spectrometry analysis of collision-induced dissociation revealing the tandem mass spectrum of a PPI peptide (A) HLA-A*1101 Epitope PPI_{80-88} (LALEGSLQQK), (B) HLA-B*3801 Epitope PPI_{5-14} (MRLLPLLALL) and (C) HLA-B*3801 Epitope PPI_{33-41} (SHLVEALYL) . The correct identity of the peptide was proven by tandem mass spectrometry of the synthetic compound. The table lists the amino acid sequence of the peptide with the expected b- and y-fragment ions (fragment ions extending from the amino- and carboxyl terminus respectively). Observed fragment ions are underlined.

Supplementary Figure 2 B) HLA-B*3801 Epitope PPI_{5-14}

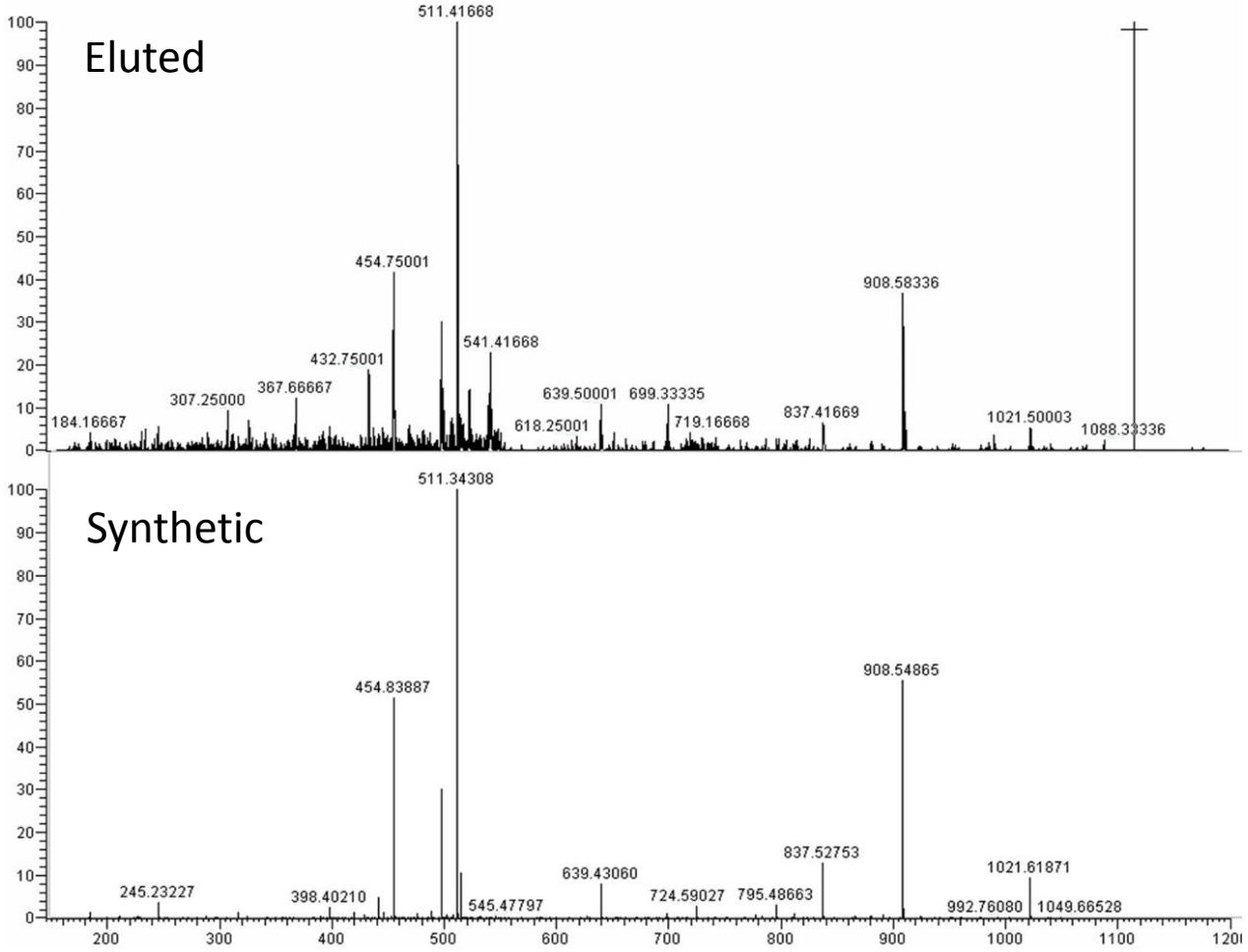

b_n ions	132	288.1	401.2	514.3	611.4	724.5	837.5	908.6	1021.7	1134.7
Peptide	M	R	L	L	P	L	L	A	L	L
y_n ions	1177.8	1021.7	865.6	752.5	639.4	542.4	429.3	316.2	245.2	132.1

Supplementary Figure 2 C) HLA-B*3801 Epitope PPI_{33-41}

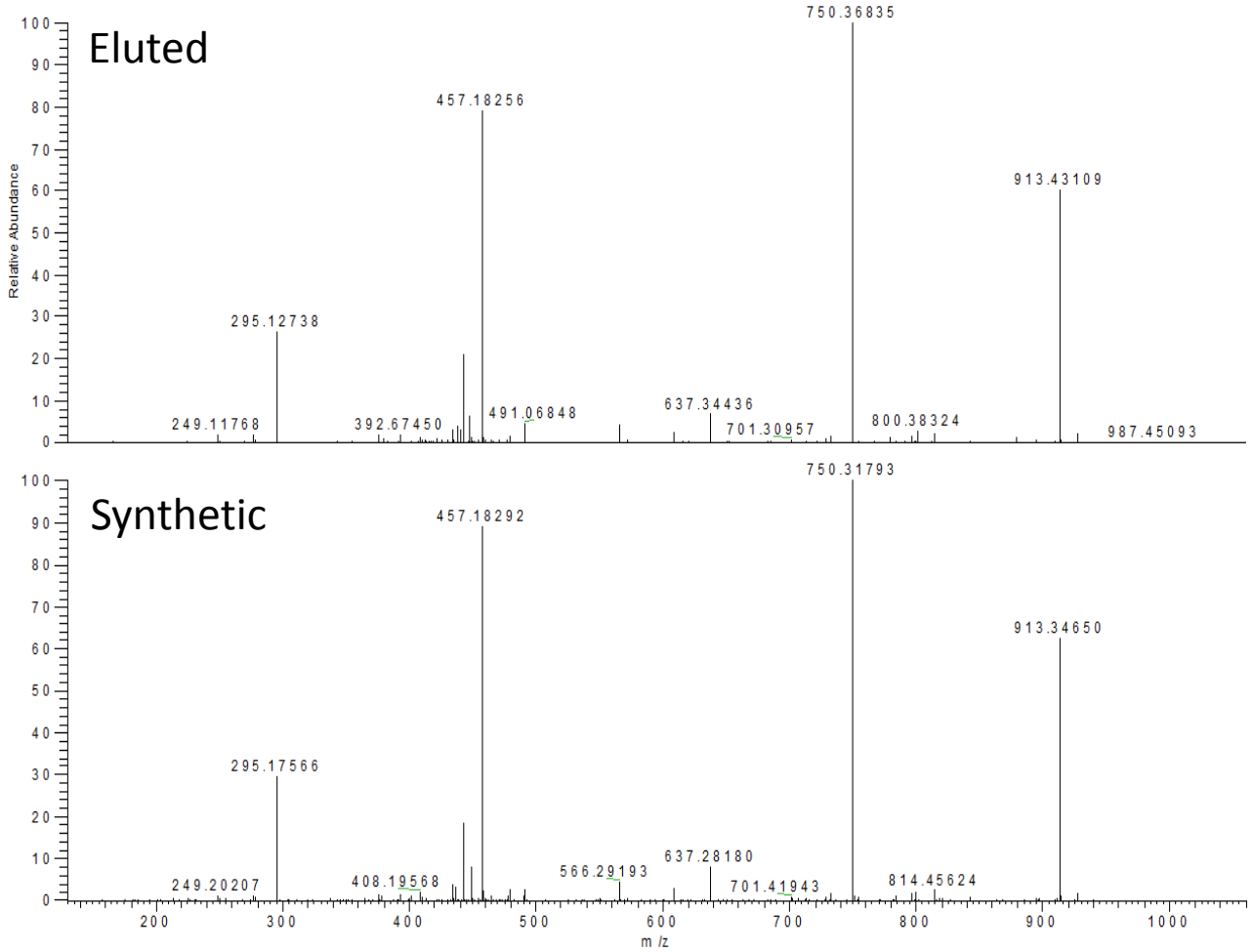

b_n ions	88	225.1	338.2	437.3	566.3	637.3	750.4	913.5	1044.6
Peptide	S	H	L	V	E	A	L	Y	L
y_n ions	1044.6	957.5	820.5	707.4	608.3	479.3	408.2	295.2	132.1

Supplementary Figure 3

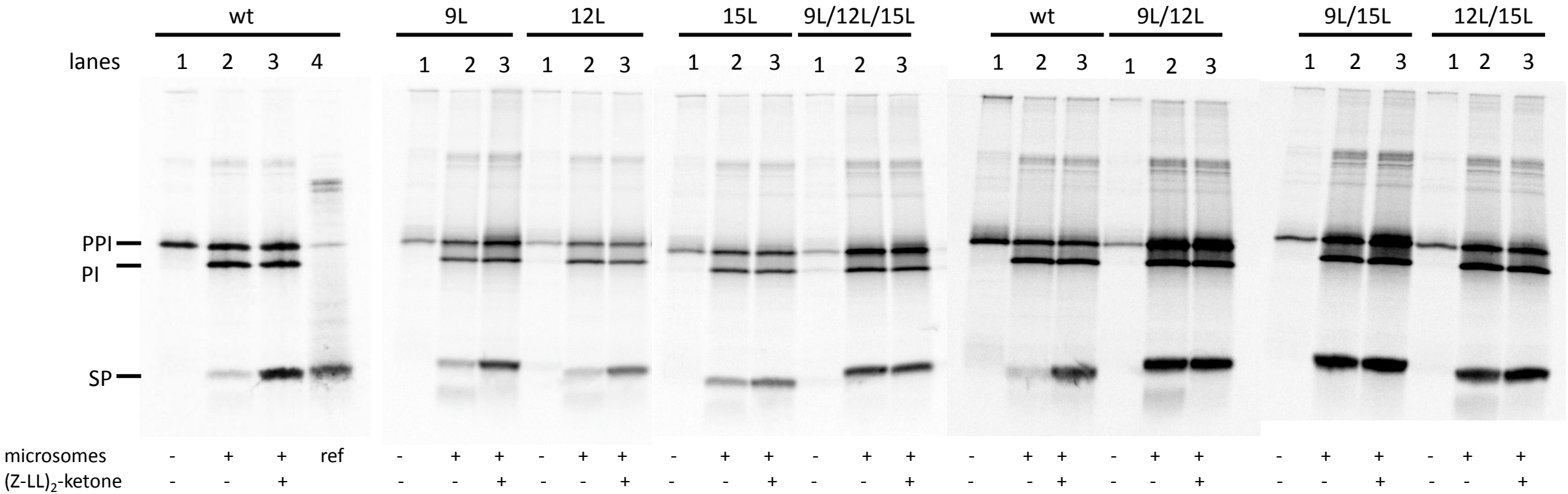

Legend Supplementary Figure 3: **Processing of the PPI signal peptide in microsomes.** *In vitro* translation of wt PPI mRNA or mutant PPI mRNA (P9L, A12L, A15L) in the absence (lanes 1) or in the presence of ER-derived microsomes (lanes 2 and 3) and SPP inhibitor $(Z\text{-}LL)_2$-ketone (lanes 3). Microsomes were isolated and analyzed by SDS-PAGE, and radiolabeled proteins visualized by phosphorimaging. Lane 4, *in vitro*-translated reference. Images are representative images of n=2, apart from wt where n=5. Equal translocation efficiency and PPI precursor availability for processing was controlled by comparing the amount of proinsulin between conditions.

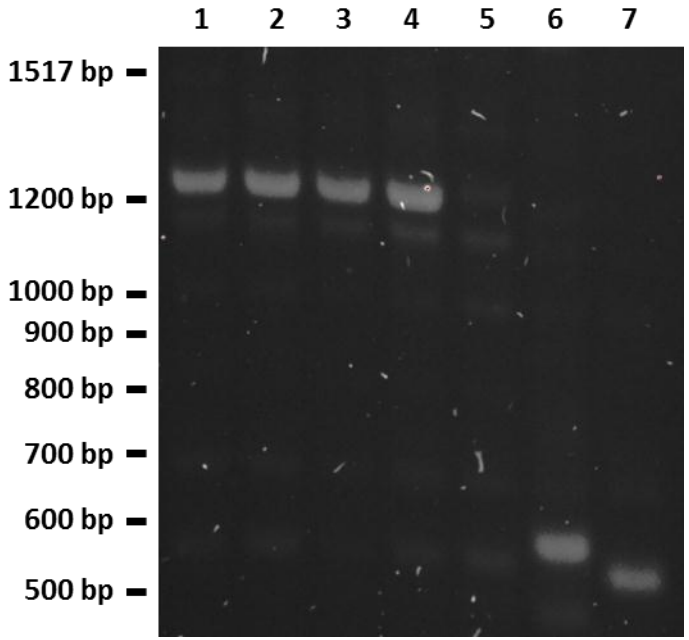

Lane	Cell line
1	K562-A2
2	K562-A2-PPI
3	K562-A2-PPI-Mock 1
4	K562-A2-PPI-Mock 2
5	K562-A2-PPI-SPPko 1
6	K562-A2-PPI-SPPko 2
7	K562-A2-PPI-SPPko 3

Legend Supplementary Figure 4: **Validation of SPP knockout (truncation) by PCR**. Within the K562-A2-PPI cells line the SPP gene was truncated using CRISPR-Cas9 directed double targeting of each exon at the start and end of the gene. Simultaneous targeting leads to truncation of the gene in effect leading to functional gene knockout. Length of the gene was assessed using PCR with SPP specific primers on cDNA generated from isolated mRNA from the cell lines. WT (lane 1 and 2) and mock transfected (lane 3 and 4) cell lines harbour full length SPP, whereas reduction (lane 6 and 7) in size or abrogation (lane 5) was observed for cell lines with effective CRISPR-Cas9 targeting of SPP.

Supplementary Figure 5

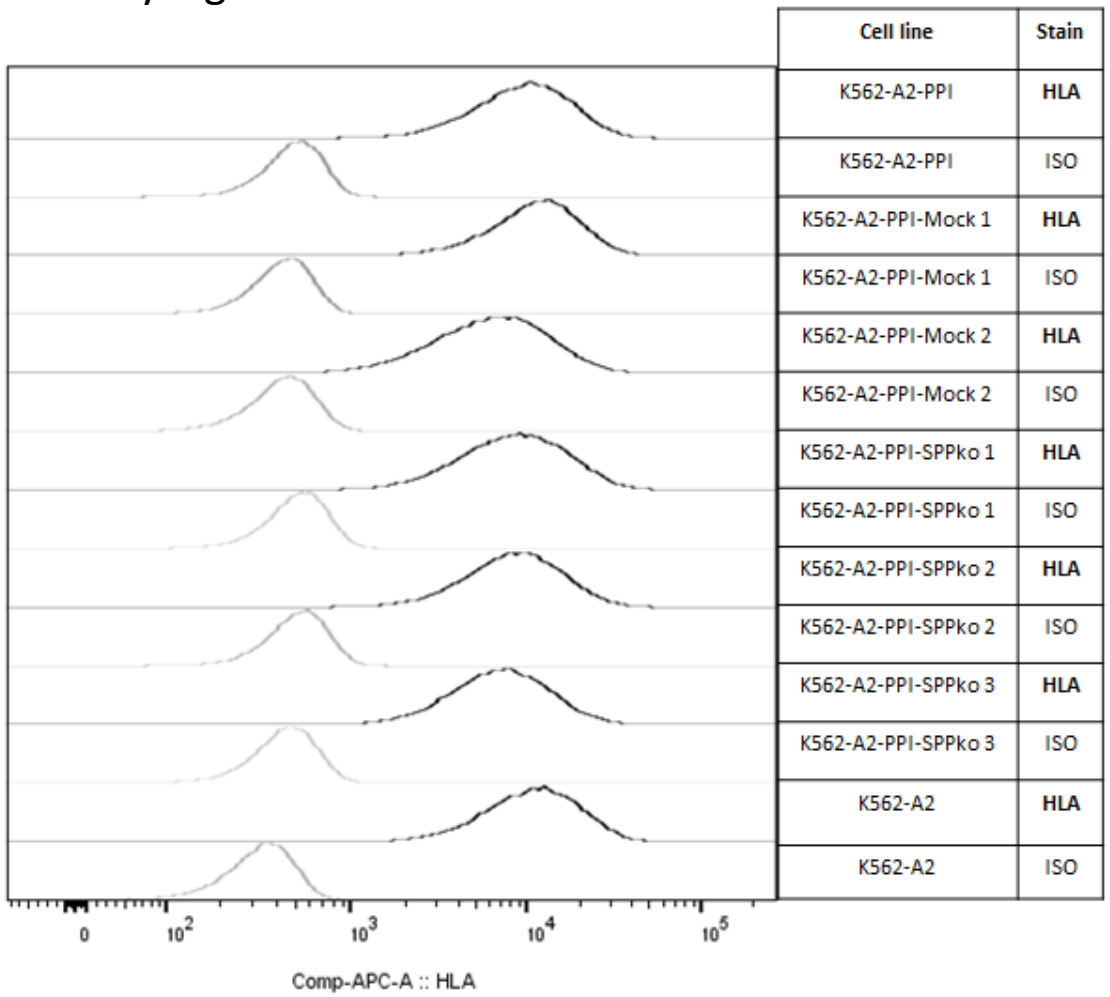

Legend Supplementary Figure 5: **HLA class I surface expression on Mock and SPPko cell lines**. Cell lines were stained with anti-pan HLA class I antibody (HLA, black line) and corresponding isotype control (ISO, grey line) antibody. Levels of surface HLA expression are similar for each experimental condition (WT, mock and SPP knockout).

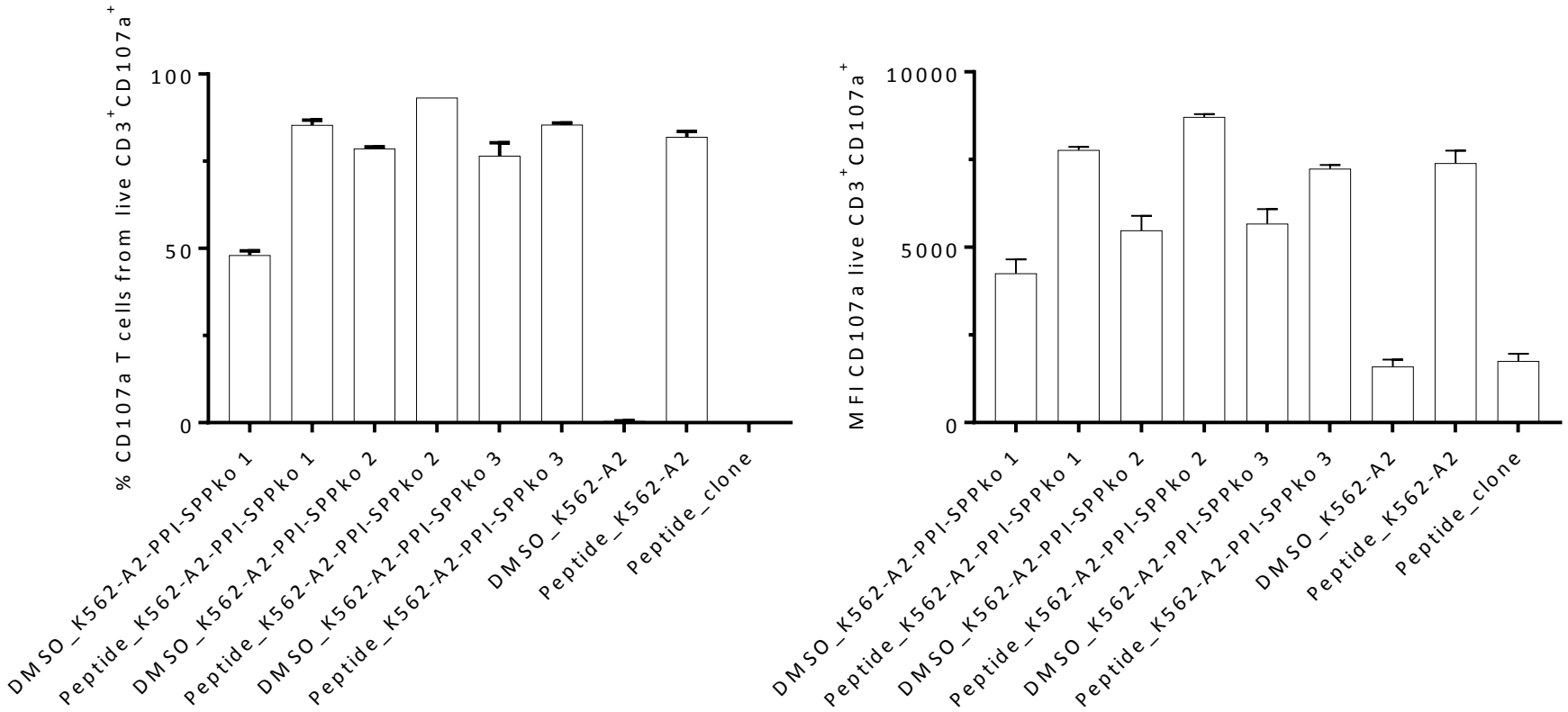

Legend Supplementary Figure 6: **Pulsing SPPko cells with cognate peptide rescues their phenotype**. K562-A2 and K562-A2-PPI-SPPko cell lines were pulsed for 1 hour with 10uM/ml peptide or peptide diluent (DMSO) prior to co-culture with T cell clone specific for PPI_{15-24}-HLA-A0201. T cell activation was assessed by CD107a expression. For each SPPko cell line, peptide pulsing leads to increased T cell activation as evidenced by both increases in percentage expression of CD107a (left) and median fluorescence intensity of CD107a (right) with comparable levels in the pulsed WT K562-A2 cell line. Three independent experiments.

Supplementary Figure 7

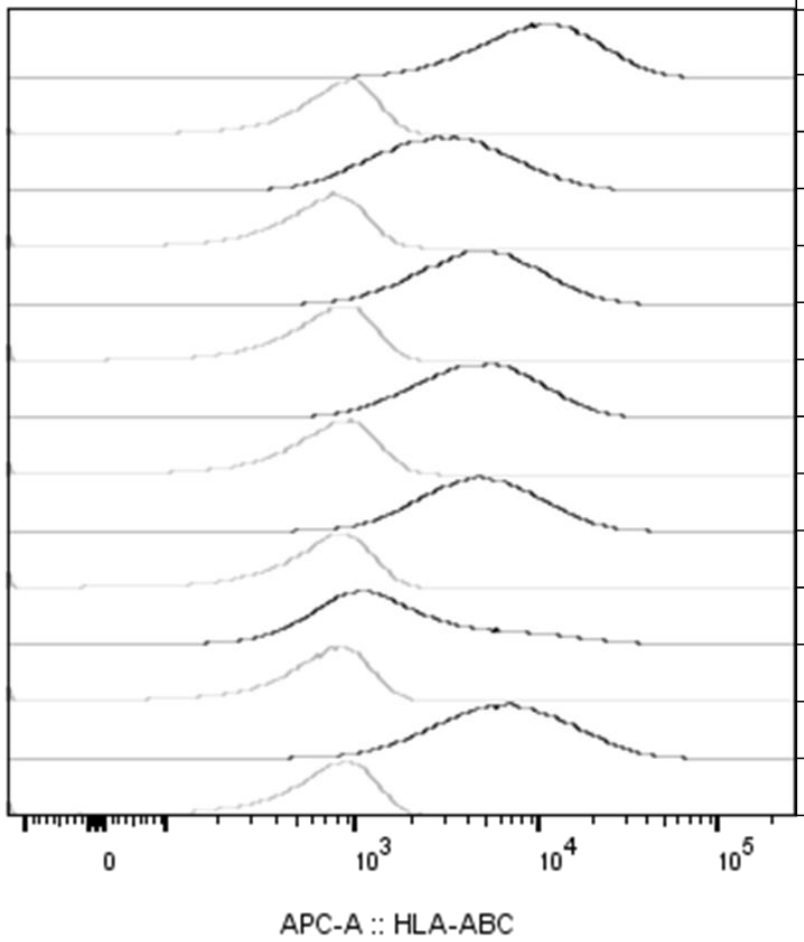

siRNA	Stain	MFI
Scramble	**HLA**	**9774**
Scramble	ISO	797
TAP1	**HLA**	**2909**
TAP1	ISO	655
TAP2	**HLA**	**4683**
TAP2	ISO	715
ERAP1	**HLA**	**4559**
ERAP1	ISO	740
ERAP2	**HLA**	**4694**
ERAP2	ISO	702
B2m	**HLA**	**1348**
B2m	ISO	691
Untreated	**HLA**	**8231**
Untreated	ISO	738

Legend Supplementary Figure 7: **HLA class I expression in siRNA experiments.** Surface HLA-ABC (W6/32 clone) expression on b2M, ERAP1, ERAP2, TAP1, TAP2, scramble knockdown treated and untreated K562-A24-PPI respectively (HLA, black line) and isotype control (ISO, grey line). Median Fluorescence Intensity (MFI) of HLA staining is shown.

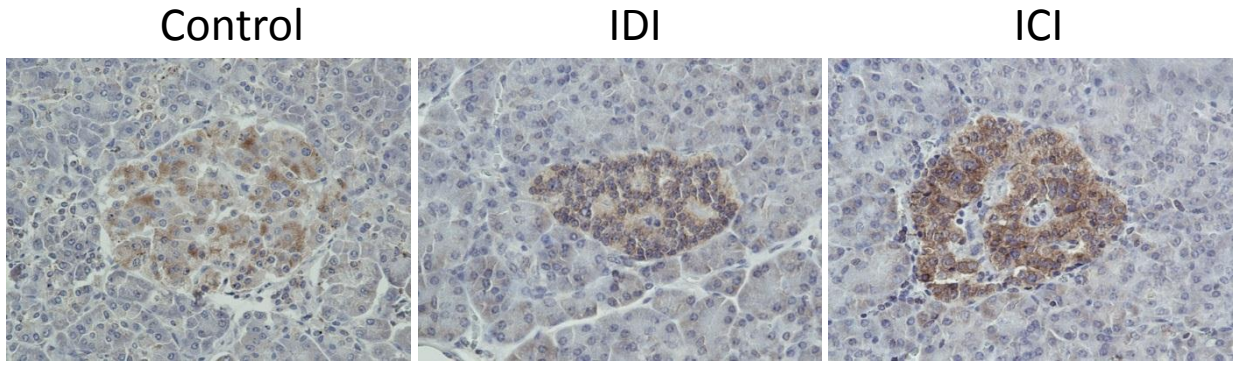

Legend Supplementary Figure 8: **Representative immunohistochemistry staining of ERAP.** Representative immunohistochemistry staining of ERAP on pancreas samples from patients with type 1 diabetes (n=3) and a representative control sample. ERAP is expressed in all islet cells irrespective of sample source and pancreas samples from type 1 diabetes patients show similar expression in insulin-deficient islets (IDI) and insulin-containing islets (ICI). These data suggest that ERAP expression is not significantly altered in the islets of patients with type 1 diabetes.

Supplementary Figure 9

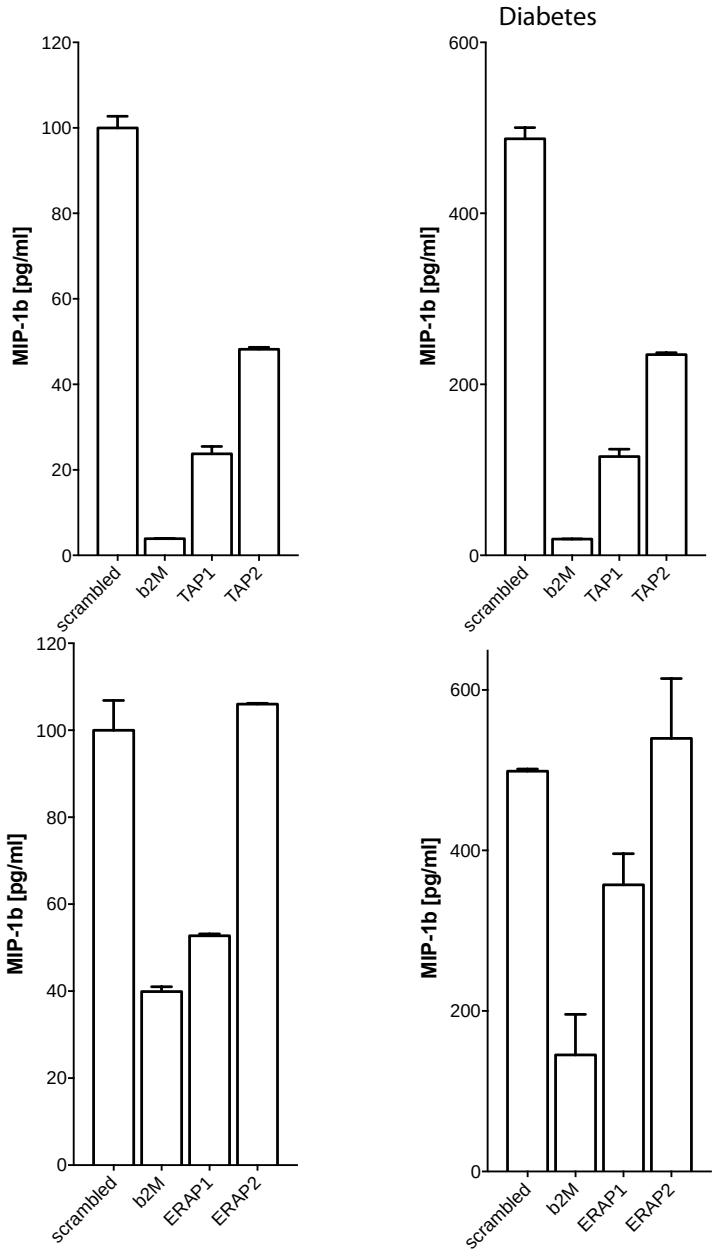

Legend supplementary Figure 9 : **MIP-1β in siRNA experiments.** MIP-1β production of HLA-A2402-restricted PPI_{3-11} specific CD8 T cell clone 4C6 upon co-culture with *β2M*, *TAP1*, *TAP2*, genes (top panel) and *ERAP1*, *ERAP2* gene (bottom panel) knockdown in K562-A24-PPI cells. Two independent experiments.

References

1. Eichmann M, de Ru A, van Veelen PA, Peakman M, Kronenberg-Versteeg D: Identification and characterisation of peptide binding motifs of six autoimmune disease-associated human leukocyte antigen-class I molecules including HLA-B*39:06. Tissue antigens 2014;84:378-388
2. The UniProt C: UniProt: the universal protein knowledgebase. Nucleic Acids Res 2017;45:D158-D169
3. Rammensee H, Bachmann J, Emmerich NP, Bachor OA, Stevanovic S: SYFPEITHI: database for MHC ligands and peptide motifs. Immunogenetics 1999;50:213-219